UNIVERSIDADE DE LISBOA
FACULDADE DE CIÊNCIAS
DEPARTAMENTO DE BIOLOGIA VEGETAL

Investigating striatal functions of Foxp1 in motor-sequence learning, automatisation of behaviour and social interaction

Sandra Filipa Ferreira Gomes

Mestrado em Biologia Molecular e Genética

Dissertação orientada por:
Doutora Catherine French
Doutor Rui Gomes

2017

Acknowledgements

"Agir, eis a inteligência verdadeira. Serei o que quiser. Mas tenho que querer o que for. O êxito está em ter êxito, e não em ter condições de êxito. Condições de palácio tem qualquer terra larga, mas onde estará o palácio se não o fizerem ali?" *(Fernando Pessoa)*

To the ones that always have had the strength to support and encourage my dreams

Abstract

Neurodevelopmental disorders are conditions of the brain function that may affect emotions, learning capabilities, memory and the control of the nervous system. Autism spectrum disorders are included in this growth impairments group. Their global prevalence has increased substantially (it is estimated that around 10 in 1000 people are now affected worldwide) and this has made it an urgent health issue to be studied. Autism spectrum disorders have a strong genetic component, with multiple genes usually contributing. However, in a minority of cases, disruptions of a single gene can result in disease. The forkhead box P subfamily is involved in many developmental and differentiation processes in the lung, heart, gut and central nervous system (transcription factor Forkhead box P1, P2 and P4), and are also involved in the immune system (transcription factor Forkhead box P3). Disruptions of the transcription factor Forkhead box P1 have been linked with autism spectrum disorders and intellectual disability. The protein FOXP1 is highly expressed in the cortex, hippocampus, thalamus and striatum of the human and mouse brain. Interestingly, the forkhead box P subfamily of proteins must homo- and heterodimerise to perform their transcriptional function. FOXP1 and FOXP2, also a member of the forkhead box family linked to deficits in language and speech, are both expressed in the striatum where they may function cooperatively. They have been show to interact *in vivo* and human mutations in both genes have a common phenotype: expressive language impairment.

To understand the functions of *Foxp1* in the striatum, a region of the basal ganglia implicated in motor-skill learning and automatisation of movement (dorsal striatum) and social behaviour (ventral striatum), a mouse line with striatal-specific *Foxp1* disruption was generated and combined with behavioural tasks to examine animals' behaviour. Immunohistochemistry and western blot techniques were performed to examine *Foxp1* expression in the neuronal cells of mutant animals and quantify protein levels.

Histological approaches confirmed the generation of a striatal-specific *Foxp1* knockdown mouse model, which is viable and shows normal body weight development. An overall assessment of motor coordination, balance and evaluation of motor-skill learning were studied and no gross motor impairment was observed. Striatal-specific *Foxp1* knockdown mice also learn and perform sequences of lever-presses normally. The sociability and preference for novelty were tested and seemed normal. Although the deletion in dorsal striatum was almost complete, which strengthens the motor function data, significant amount of Foxp1 protein remained in ventral striatum, which did not allow conclusions about the relation between Foxp1 loss and social behaviour.

To evaluate a possible relation between *Foxp1* and *Foxp2* genes, a new mouse line with global disruption of *Foxp1* and *Foxp2* was created and showed pronounced motor-skill learning deficits, although their body weight development was normal until day 21. Although these data are consistent with a cooperative role for Foxp1 and Foxp2 in motor-skill learning, at this stage it is not possible dismiss the possibility that we are affecting two pathways that independently contribute to motor-skill learning.

The striatal-specific *Foxp1* knockdown line allows to observe some interesting characteristics but future studies can be conducted with different tasks and mouse models, for example, using the new mouse line with global disruption of *Foxp1* and *Foxp2* to investigate social deficits or even deleting the *Foxp1* gene in adulthood with viral injections in the nucleus accumbens to investigate social behaviour.

Keywords

Neurodevelopmental disorders
Autism spectrum disorders
Foxp1 knockdown mice
Striatum

Resumo

As desordens do desenvolvimento neuronal são condições da função cerebral que podem afetar as emoções, a capacidade de aprendizagem, a memória e o próprio controlo do sistema nervoso. Os gânglios basais constituem o grupo de núcleos subcorticais primariamente responsáveis pelo controlo motor, pela aprendizagem motora, por executar funções e comportamentos e ainda pelas emoções. Disrupções nesta região do cérebro conduzem a várias desordens no movimento e na atividade neuronal. As desordens do espectro do autismo, um dos exemplos mais comuns de doenças do desenvolvimento neuronal, exibem fenotipicamente uma função intelectual, motora e comportamental alterada. A sua prevalência global tem aumentado substancialmente (estima-se que 10 em cada 1000 indivíduos sejam afetados mundialmente), o que tem enfatizado a urgência do estudo deste problema de saúde global. Em Portugal, embora inferior à mundial, a prevalência global da doença é de 0,92 em cada 1000 crianças em idade escolar. Algumas diferenças regionais são encontradas nos Açores, onde a prevalência é de 1,56 em cada 1000 crianças em idade escolar. O estudo destas doenças emergentes é relevante não só ao nível de um possível diagnóstico cada vez mais precoce como ao nível do desenvolvimento de novos tratamentos, mais dirigidos e personalizados, que permitam aumentar a qualidade de vida dos doentes e a diminuição do custo destas patologias, tanto para a família como para a sociedade.

As doenças do espetro do autismo têm uma forte componente genética, com múltiplos genes envolvidos. Embora alguns casos raros de um único gene envolvido estejam já descritos, a hipótese da interação de diferentes proteínas parece ser a melhor aceite. Mutações no fator de transcrição da família de proteínas de ligação ao DNA, também conhecidas por proteínas *forkhead box*, bem como alterações nos padrões de expressão do gene *Foxp1*, têm sido associadas às doenças do espetro do autismo, nomeadamente na regulação da excitabilidade dos neurónios espinhosos médios, a défices na vocalização ultrassónica e a outras patologias que afetam a capacidade intelectual. Todas as funções que as proteínas desempenham no cérebro continuam ainda por desvendar. Sabe-se, no entanto, que esta família de proteínas está associada a vários processos cruciais no desenvolvimento e diferenciação (fatores de transcrição Foxp1, Foxp2 e Foxp4), bem como a processos envolvidos no sistema imunitário (fator de transcrição Foxp3). A proteína FOXP1 é altamente expressa em três regiões do cérebro humano e de roedores: córtex, hipocampo e estriado. O gene *Foxp1* é regulado pelo gene *Foxp2*, também membro da subfamília de proteínas *forkhead box* e associado a défices cognitivos na linguagem e no discurso. É conhecida a interação entre os dois genes em processos biológicos e o seu fenótipo comum, evidenciado essencialmente ao nível de défices na expressão da linguagem. Ambos são expressos a partir do dia embrionário 12,5, permanecendo durante a fase adulta.

Para compreender as funções do gene *Foxp1* no estriado, uma região dos gânglios basais que está implicada na aprendizagem da sequência motora e na automatização do movimento (zona dorsal do estriado) e no comportamento social (zona ventral do estriado), foi realizada uma abordagem de supressão do gene especificamente no estriado. Foram realizadas abordagens de imunohistoquímica e *western blot* para visualização da expressão das proteínas ao nível celular e para a sua quantificação proteica, respetivamente. A linha de ratinho criada foi submetida a diferentes tarefas comportamentais, permitindo observar as microestruturas envolvidas no comportamento animal *in vivo*, tanto ao nível do movimento como do processo de socialização.

A abordagem histológica confirmou a criação de um modelo de ratinho com diminuição da expressão do gene *Foxp1* no estriado, que é viável e revela um normal desenvolvimento. A avaliação da coordenação motora, do balanço e a avaliação da capacidade de aprendizagem da sequência motora mostraram que não existe défice ao nível da função motora quando a expressão do gene é reduzida. A linha de ratinho criada também revelou uma capacidade de aprendizagem e performance da sequência motora normal. O comportamento social foi estudado, tanto ao nível do processo de socialização como

ao nível da preferência pela novidade social após um primeiro contacto com um indivíduo conhecido. O modelo animal não evidenciou diferenças significativas nestas abordagens. Apesar da deleção na região dorsal do estriado ter sido quase completa, o que fortalece os resultados obtidos no que concerne à função motora, a deleção foi apenas substancial na região ventral do estriado, o que não permite concluir com este modelo acerca da relação da perda de função da proteína e o comportamento social.
De modo a avaliar uma possível interação entre os genes *Foxp1* e *Foxp2*, uma nova linha transgénica de ratinho foi criada, na qual foi introduzida uma disrupção global de ambos os fatores de transcrição. Este novo modelo revelou interessantes défices ao nível da função motora, apesar do seu desenvolvimento ser normal até aos 21 dias de idade. Apesar destes resultados serem consistentes com uma possível cooperação funcional de *Foxp1* e *Foxp2* na aprendizagem da capacidade motora, não é possível eliminar a hipótese deste procedimento poder estar a ser influenciado por duas vias que independentemente contribuem para o processo.
A abordagem com o modelo biológico na qual o gene *Foxp1* está especificamente suprimido no estriado permitiu observar características interessantes mas estudos futuros poderão ser conduzidos com outros modelos e com a utilização de diferentes tarefas comportamentais como, por exemplo, a utilização da nova linha de ratinho com a disrupção global de *Foxp1* e *Foxp2* em tarefas de comportamento mais específicas para o processo de interação de diferentes entidades sociais, ou mesmo a supressão localizada do gene *Foxp1* em regiões específicas do estriado de ratinhos adultos, com recurso a técnicas de injeção viral.

Palavras-chave

Desordens do desenvolvimento neuronal
Desordens do espetro do autismo
Gene *Foxp1*
Estriado

Contents

Figures and Tables

Abbreviations

ANOVA – Analysis of variance
ASDs – Autism spectrum disorders
bp – Base pair
Control(s) – Littermates without Cre-mediated disruption of the *Foxp1* gene (*Foxp1*$^{flox/flox}$; *Rgs9-Cre*$^{-}$ and *Foxp1*$^{flox/+}$; *Rgs9-Cre*$^{-}$)
DAB – 3,3,diaminobenzidine substrate
dHet – Mice heterozygous for *Foxp1-Δ11-12* (*Foxp1*$^{Δ11\text{-}12/+}$) and *Foxp2-S321X* (*Foxp2*$^{S321X/+}$)
dMSNs – Striatal medium spiny projection neurons that constitute the striatonigral or direct pathway
DSM III – Diagnostic and Statistical Manual of Mental Disorders III
E – Embryonic day
FOX – Forkhead box family (see footnote [1] on page 4)
FOXP – Forkhead box protein (see footnote [1] on page 4)
FOXP1 – Forkhead box protein 1 (see footnote [1] on page 4)
Foxp1 heterozygous – Mice heterozygous for the *Foxp1* conditional allele with disruption of the gene mediated by Cre recombinase (*Foxp1*$^{flox/+}$; *Rgs9-Cre*$^{+}$)
Foxp1 homozygous – Mice homozygous for the *Foxp1* conditional allele with disruption of the gene mediated by Cre recombinase (*Foxp1*$^{flox/+}$; *Rgs9-Cre*$^{+}$)
Foxp1-Δ11-12 – Mouse line with the disruption of *Foxp1* in germline
Foxp1$^{flox/flox}$ mice – Mice homozygous for the *Foxp1* conditional allele
FOXP2 – Forkhead box protein 2 (see footnote [1] on page 4)
Foxp2-S321X – Mouse line with the disruption of *Foxp2*
FOXP3 – Forkhead box protein 3 (see footnote [1] on page 4)
FOXP4 – Forkhead box protein 4 (see footnote [1] on page 4)
FR8 – Fixed-ratio 8 schedule
H_2O_2 – Hydrogen peroxide
Het1 – Mice heterozygous for *Foxp1-Δ11-12* with wild-type *Foxp2* alleles
Het2 – Mice heterozygous for *Foxp2-S321X* and with wild-type *Foxp1* alleles
HRP – Horseradish peroxidase
ImageJ – Image Processing and Analysis in JAVA
iMSNs – Striatal medium spiny projection neurons that constitute the striatopallidal or indirect pathway
IPIs – Inter-press intervals
MAD – Median absolute deviation
MSNs – Striatal medium spiny projection neurons
n – Number of subjects in each condition
ON – Overnight
PBS – Phosphate buffered saline
PCR – Polymerase chain reaction
PFA – Paraformaldehyde
Rgs9-Cre^{+} mice – Mice expressing Cre recombinase under control of the *Rgs9* promoter
RT – Room temperature
SEM – Standard error of the mean
TAE – Tris-acetate-EDTA (ethylenediaminetetraacetic acid)
TBS – Mixture of tris-buffered saline
TBST – Mixture of tris-buffered saline (TBS) and Polysorbate 20 (Tween 20)
Tregs – Regulatory T cells

UV – Ultraviolet light radiation
WHO – World Health Organisation
WT – Wild type
x – Times

1. Introduction

1.1. Impact of neurodevelopmental disorders

According to the World Health Organisation (WHO), neurodevelopmental disorders involve a group of conditions with onset in infancy or childhood, characterised by the impairment or delay in functions related to the central nervous system formation, development and maturation (World Health Organization, Geneva 2013). These disorders may affect a single area of development (specific developmental disorders of speech and language, of scholastic skills, and/or motor function) or several areas (pervasive developmental disorders and intellectual disability) (World Health Organization, Geneva 2013).

1.1.1. Autism spectrum disorders

The word "autism" was initially used to describe a subset of schizophrenia patients who were especially withdrawn and self-absorbed. In 1938 some cases of children with similar symptoms were reported but the first cases of "early infantile autism" were only described in 1943 (Kanner 1943). In 1980, "infantile autism" was listed in the Diagnostic and Statistical Manual of Mental Disorders III (DSM III) (American Psychiatric Association 1980), and officially separated from childhood schizophrenia. Since then it has come to be recognised as a neurodevelopmental disorder, with varying degrees of severity, and a strong genetic and biological basis (Boat *et al.* 2015).

Autism spectrum disorders (ASDs) are now defined as group of heterogeneous neurodevelopmental conditions such as autism, childhood disintegrative disorder and Asperger syndrome, characterised by diminished sociability, impaired communication, restricted interests and stereotypic behaviours (Chen *et al.* 2015; World Health Organization, Geneva 2013). The symptoms include a variable mixture of impaired capacity for reciprocal socio-communicative interaction and a restricted stereotyped repetitive repertoire of interests and activities (World Health Organization, Geneva 2013).

Neurodevelopmental impairments in communication, social interaction and unusual ways of perceiving and processing information can seriously hinder daily functioning of people with ASDs and severely impede their educational and social attainments. Together with the increasing prevalence of ASDs diagnosis this has made it an urgent health issue to be studied (World Health Organization, Geneva 2013).

1.1.2. Prevalence and genetics of autism

Epidemiological studies conducted over the past fifty years have shown that the global prevalence of ASDs diagnosis has increased, particularly over the last two decades. It is estimated that around 10 persons in 1000 is now affected worldwide (Elsabbagh *et al.* 2012). There are many possible explanations for this apparent increase in prevalence, namely improved awareness, expansion of diagnostic criteria, better diagnostic tools or improved reporting (World Health Organization, Geneva 2013).

In Portugal, the reported frequency is lower, around 1 child in 1000 at school age (although the data are less recent). The Portuguese isles Açores show an increased rate of 1,56 children in 1000 at school age in comparison with the continental rate of 0,92 children in 1000 at school age (Table 1.1) (Oliveira *et al.* 2007).

Table 1.1. Prevalence of autism in Portugal. Number of children in Portugal surveyed by teachers, selected for assessment, observed and diagnosed with ASDs, and prevalence estimates per 1000 children for school-year 1999 to 2000 by geographic region. 163 cases of children were not represented for unknown reasons. None of these children were referred with four or more positive items in questionnaire. The values shown have a confidence interval of 95%. This table was adapted from (Oliveira *et al.* 2007).

Geographic region	Prevalence of ASD per 1000 children
Norte	0,60 (0,50 – 0,75)
Centro	1,25 (0,96 – 1,50)
Lisboa e Vale do Tejo	1,23 (1,00 – 1,40)
Alentejo	0,70 (0,30 – 1,10)
Algarve	0,24 (0,30 – 0,50)
Mainland total	0,92 (0,81 – 1,00)
Azores	1,56 (0,80 – 2,30)

The earliest prevalence studies also found a consistent sex difference, with boys being 3 to 4 times more likely to have autism than girls (Boat *et al.* 2015) (DiLuca *et al.* 2014) (World Health Organization, Geneva 2013).

It is known that there is a strong genetic component to ASDs, but the situation is usually complex with multiple genes contributing to the prevalence of the disorder (Geschwind *et al.* 2015). However, in a minority of cases disruptions of a single gene can result in ASDs, for example mutations in the *NF1* gene cause ASDs as well as other neurodevelopmental problems (Vogel *et al.* 2017). These monogenic disorders provide an entry point into the underlying molecular and biological mechanisms.

1.2. Functional neuroanatomy of the basal ganglia

The basal ganglia are a group of structures found deep within the cerebral hemispheres and the brainstem that include the caudate nucleus, putamen, globus pallidus, subthalamic nucleus and substantia nigra. The caudate and putamen form the striatum, and the globus pallidus and substantia nigra are each made up of multiple nuclei. The main function of the basal ganglia is processing movement related information (intensity, direction and sequence). The other functions are associated with emotion, motivation and cognitive functions (Kalat 2012).

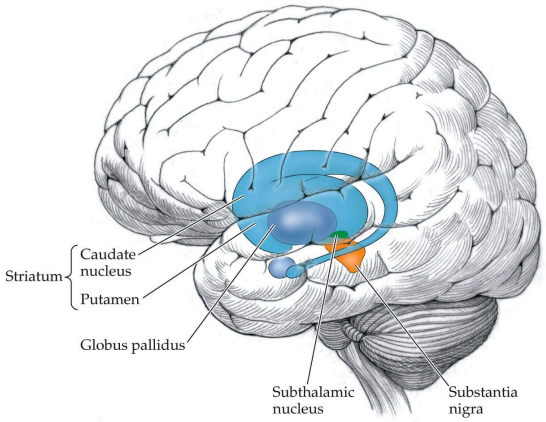

Figure 1.1. Neuroanatomy of the basal ganglia (Kalat 2012).

The cerebral cortex, responsible for memory, attention, consciousness, language or even perception, receives information and sends this stimulus to the caudate nucleus or putamen (main input nuclei of the basal ganglia). The globus pallidus and substantia nigra constitute the main output nuclei and send

projections out, usually by the thalamus, to the cortex and the brainstem (Matthews 2001; Kalat 2012). The basal ganglia pathways have been studied in the last decades and the classical view is that there are different circuits in the basal ganglia that promote and inhibit movement. In general, when a signal or stimulus to initiate movement is sent from the cortex to the basal ganglia it follows a circuit in the basal ganglia known as the direct pathway, which leads to the silencing of neurons in the globus pallidus. This allows movement to initiate, once the thalamus is inhibited by the globus pallidus. The indirect pathway of the basal ganglia involves the subthalamic nucleus and leads to increased suppression of unwanted movements (Squire *et al.* 2013; Purves *et al.* 2012). However, it should be noted that recent studies have shown that both pathways are co-active during movement suggesting that concerted activity the two is required for proper action performance (Klaus *et al.* 2017; Tecuapetla *et al.* 2014).

1.2.1. Striatal function, morphology and organisation

The striatum is a small group of structures found below the cerebral cortex that consists of the caudate (dorsomedial striatum in rodents), putamen (dorsolateral striatum in rodents), and ventral striatum (consists of nucleus accumbens and olfactory tubercle). This major component of the basal ganglia is crucial for reinforcement processing after an action and the different sub-regions have dissociable functions. The caudate is associated with action-outcome learning whereas the putamen is involved in stimulus response learning, and the ventral striatum in mediating motivational and affective learning (Figure 1.2) (Klaus *et al.* 2017; Tecuapetla *et al.* 2014).

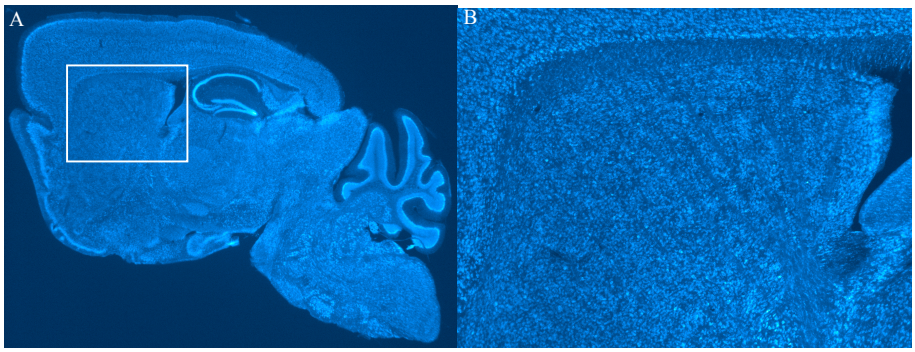

Figure 1.2. Nissl staining of a sagittal section of a C57BL/6J mouse brain. The Nissl staining is a classic nucleic acid staining method used on nervous tissue sections, where a basic dye (aniline, thionine, or cresyl violet) binds to negatively charged nucleic acids like RNA and DNA. B (magnification of 5 x) represents the region delimited by the rectangle in A (magnification of 1,25 times (x)), specifically the dorsal striatum region.

The dopamine D1 receptor-expressing striatal medium spiny projection neurons (MSNs) (Figure 1.3) that constitute the striatonigral or direct pathway (dMSNs) and the dopamine D2 receptor-expressing MSNs that constitute the striatopallidal or indirect pathway (iMSNs) can cooperate and are the two subpopulations of MSNs, which constitute mainly the striatum together with a smaller number of distinct classes of interneurons (Vicente *et al.* 2016; Marzluff *et al.* 2012; Matthews 2001; Squire *et al.* 2013).

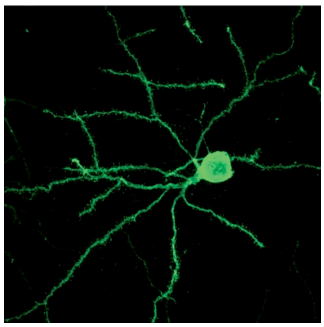

Figure 1.3. MSNs represent 95% of the total number of striatal neurons. The phenotype is characterised by medium size (around 20 millimetres (mm) in diameter) with multipolar stellate cells with radially oriented dendrites, which are covered by dendritic spines, small postsynaptic specializations (Lanciego *et al.* 2012).

1.3. The forkhead box family

The Forkhead box (FOX) proteins are an evolutionarily ancient family of transcription factors characterised by a highly conserved forkhead DNA-binding domain with 110 amino acids (Golson *et al.* 2016). The FOXP subfamily proteins (FOXP1-4)[1] are unique in that they must homo- or heterodimerise to perform their transcriptional function, a process which is mediated through the conserved zinc-finger and leucine-zipper domains (Figures 1.4 and 1.5) (Golson *et al.* 2016). They have a wide range of important biological functions in many developmental and differentiation processes: FOXP1, FOXP2 and FOXP4 are involved in the lung, heart, gut and central nervous system; FOXP3 is linked with the regulatory T cells (Tregs) of the adaptive immune system (Golson *et al.* 2016). The functional importance of this subfamily has been recognised because mutations in these genes cause different diseases. For example, mutations in the dimerization domain of FOXP3 result in IPEX syndrome (immune dysregulation, polyendocrinpathy, enteropathy, X-linked syndrome) (Golson *et al.* 2016).

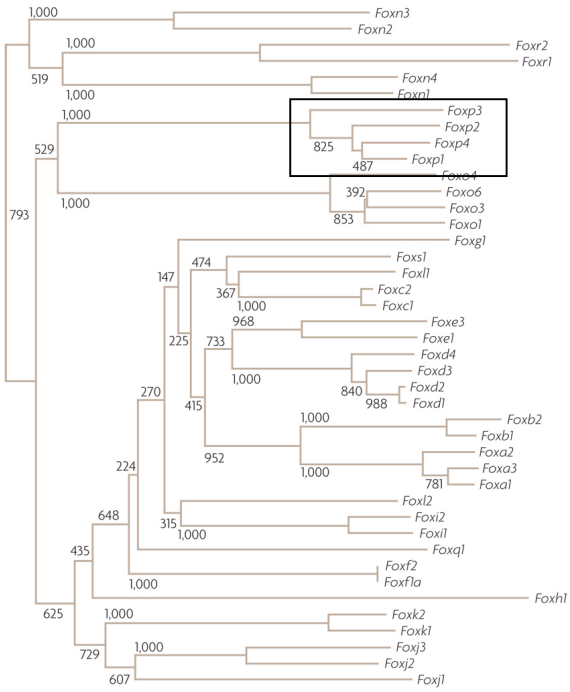

Figure 1.4. Evolution of tree mouse of Fox proteins. The rectangle represents the members of Foxp subfamily: Foxp1-4 (Hannenhalli *et al.* 2009).

[1] The standard nomenclature is FOXP for humans, Foxp for mice and FoxP for other species, or when referring to several species; genes and RNA are italicised.

The *FOXP1* and *FOXP2* genes have generated interest because of their links with neurodevelopmental disorders (Bacon *et al.* 2012). Disruptions of the *FOXP2* gene cause a severe speech and language disorder, which has been characterised in detail in the KE family (Vargha-Khadem *et al.* 2005; Morgan *et al.* 2016). Affected family members carry a missense mutation in the DNA-binding domain of *FOXP2* which is responsible for wide-ranging impairments in oral and written language which impact on both receptive and expressive skills (Figure 1.5) (Watkins *et al.* 2002; Lai *et al.* 2001). A core phenotype of the disorder is developmental verbal dyspraxia (also known as childhood apraxia of speech), where imprecise and inconsistent neural control of sequences of orofacial movements impedes development of fluent speech (Watkins *et al.* 2002).

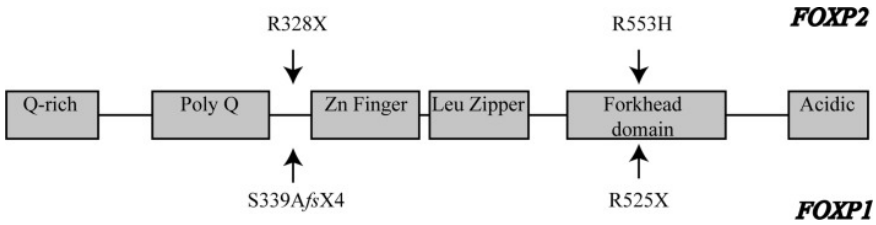

Figure 1.5. Examples of different *FOXP1* and *FOXP2* mutations described (Bacon *et al.* 2012).

More recently, it has been shown that disruptions of the *FOXP1* gene result in a broader neurodevelopmental disorder, including ASDs, speech and language impairment and intellectual disability as well as other phenotypes including sensory integration disorder and hypertelorism (Figure 1.5) (Sollis *et al.* 2016, 2017; Myers *et al.* 2017; Bacon *et al.* 2012). The similarities and differences between *FOXP1*- and *FOXP2*-related disorders are shown in (Figure 1.6).

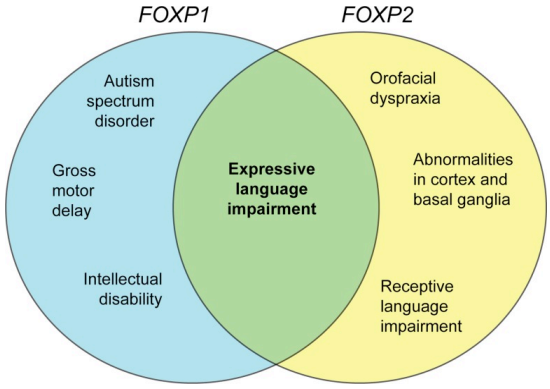

Figure 1.6. The similarities and differences between phenotypes associated with FOXP1 and FOXP2 disruptions (Bacon *et al.* 2012).

1.3.1. The role of Foxp1 in the developing brain

Studies in mice have been used to investigate functions of the Foxp2 protein and have uncovered roles in motor-skill learning and striatal synaptic plasticity (Groszer *et al.* 2008; French *et al.* 2012). However, much less is currently known about Foxp1 functions.

Foxp1 is crucial for embryonic development and regulates cardiac outflow tract, endocardial cushion morphogenesis and myocite proliferation and maturation (Wang *et al.* 2004).

In the brain, *Foxp1* expression has been detected from embryonic day (E) 12,5 in the developing telencephalon and expression persists into adulthood. The gene is expressed in the striatum, cortex (layers 3 to 5), hippocampus and thalamus (Ferland *et al.* 2003). In the adult striatum, *Foxp1* expression is found in MSNs with no expression detected in striatal interneurons (Ferland *et al.* 2003; Tamura *et al.* 2003, 2004). Expression levels are similar in D1- and D2-receptor expressing MSNs

(Vernes *et al.* 2011). It has been shown that *FOXP1* is also expressed in the developing human striatum over an equivalent gestational period and with a similar anatomical distribution to that seen in rodents (Teramitsu *et al.* 2004). Interestingly, the striatum is a brain region where *Foxp1* expression overlaps with *Foxp2* expression (Ferland *et al.* 2003), meaning that the proteins could potentially heterodimerise and function cooperatively. This was recently shown to occur *in vivo* in the songbird striatal nucleus, Area X (Mendoza *et al.* 2017).

Mice with global homozygous deletion of Foxp1 are embryonically lethal (Wang *et al.* 2004). Heterozygous mice are viable and show increased excitability of striatal MSNs and deficits in vocalisations (Araujo *et al.* 2015). Mice with brain-specific deletion of Foxp1 have also been generated and have anatomical changes in the striatum as well as electrophysiological abnormalities in the hippocampus. These animals also display additional cognitive and social deficits including altered vocalisations (Fröhlich *et al.* 2017; Bacon *et al.* 2015).

1.4. Project aims

The project "Investigating striatal functions of *Foxp1* in motor-sequence learning, automatisation of behaviour and social interaction" involves three main goals: quantify Foxp1 protein knockdown in mice with striatum-specific knockdown of *Foxp1* and littermate controls and confirm if it is striatum-specific; study of motor-sequence learning and automatisation of motor behaviour in striatum-specific *Foxp1* knockdown mice and controls; and assess social approach behaviour and preference for social novelty in striatum-specific *Foxp1* knockdown mice and controls.

2. Materials and Methods

2.1. Animals

All animal procedures were reviewed and performed in accordance with the Champalimaud Centre for the Unknown Ethics Committee guidelines and approved by the Portuguese Veterinary General Board (Direção Geral de Alimentação e Veterinária, approval 0421/000/000/2014).

Animals were maintained and bred in specific pathogen-free barrier facilities at the vivarium of Champalimaud Foundation, under a 12 hours (h) light/dark cycle, with controlled temperature and humidity (respectively 18 - 24 degrees Celsius (ºC) and 40 - 75 %). Food and water were supplied *ad libitum*, except during the operant motor-sequence learning task (see below).

Body weight was monitored during development. Male and female animals were tested at the age of 10 weeks (2 months) to 22 weeks (5 months). Mice were maintained on a mixed genetic background (majority C57BL/6J with some CD-1 and 129/Sv), which did not change during the course of the study because all experimental animals were the offspring from the same set of breeding pairs.

2.2. Generation of mutant mice

The conditional gene knockout is a technique used to eliminate a specific gene in a tissue or region in alternative to the traditional gene knockout technique, in which a gene mutation can cause embryonic death. This new conditional approach also allows the study of a gene at a specific developmental stage or in adults (Guan *et al.* 2010; Zhang *et al.* 2012; Skarnes *et al.* 2013).

Mice with a *Foxp1* conditional allele were previously generated using the targeting vector shown below (Figure 2.1) (Feng *et al.* 2010). LoxP sites flank exons encoding the key DNA-binding domain of *Foxp1*. Thus expression of Cre recombinase deletes *Foxp1* exons 11 and 12 (Figure 2.1).

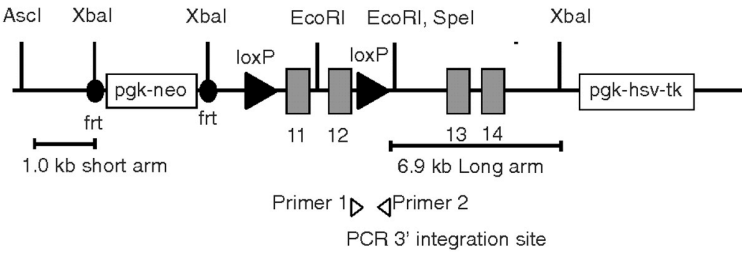

Figure 2.1. Diagram of the targeting vector containing *Foxp1* exons 11 to 14. The *Foxp1* conditional construct was designed to have short (1,0 kilobase (kb)) and long (6,9 kb) arms of homology. Cre recombinase conditionally deletes *Foxp1* exons 11 and 12 flanked by 2 loxP sites. Flp recombinase deletes the neo marker from the mouse germline (Feng *et al.* 2010).

To generate mice with *Foxp1* disrupted specifically in the striatum, mice with the *Foxp1* conditional allele ($Foxp1^{flox/flox}$ mice) (Feng *et al.* 2010) were crossed with mice expressing Cre recombinase under control of the *Rgs9* promoter, specific for striatal medium spiny neurons ($Rgs9\text{-}Cre^{+}$ mice) (Dang *et al.* 2006) (Figure 2.2).

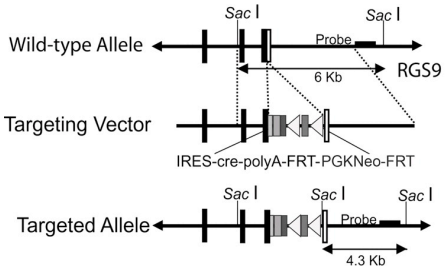

Figure 2.2. Targeting construct for the Rgs9-cre mouse. The striatum-specific Cre mouse was made by employing the restricted expression pattern of RGS9 protein, the product of a splice variant of the *Rgs9* gene that is expressed predominantly in the striatum. A *cre* gene was inserted at the 3' end of the *Rgs9* gene (Dang *et al.* 2006).

After the mice generation (Figure 2.3) the genotypes were determined by polymerase chain reaction (PCR) amplification in order to select the heterozygous mice for *Foxp1* conditional allele with the disruption of the gene mediated by Cre recombinase (*Foxp1*$^{flox/+}$; *Rgs9-Cre*$^{+}$) (abbreviated to *Foxp1* heterozygous).

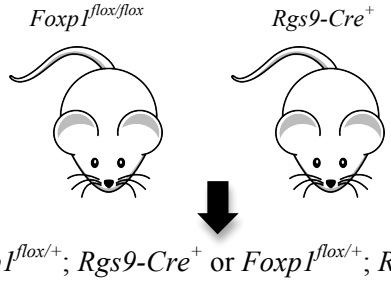

Figure 2.3. Generation of *Foxp1* heterozygous mice. *Foxp1 flox/flox* mice were crossed with *Rgs9-Cre*$^{+}$ mice. From this breeding *Foxp1* heterozygous mice were selected for the next breeding step.

Foxp1 heterozygous mice were crossed with *Foxp1 flox/flox* mice for the generation of mice without the Cre-mediated disruption of the gene (*Foxp1*$^{flox/flox}$; *Rgs9-Cre*$^{-}$ and *Foxp1*$^{flox/+}$; *Rgs9-Cre*$^{-}$) (abbreviated to Controls), and mice heterozygous and homozygous for the *Foxp1* conditional allele with the disruption of the gene mediated by Cre recombinase (*Foxp1*^{floxflox}; *Rgs9-Cre*$^{+}$, abbreviated to *Foxp1* homozygous) (Figure 2.4).

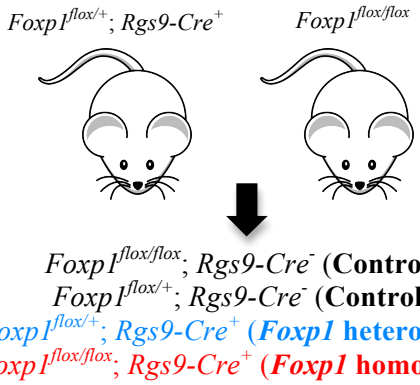

Figure 2.4. Generation of experimental animals with *Foxp1* disrupted specifically in the striatum. *Foxp1* heterozygous mice were crossed with *Foxp1*$^{flox/flox}$, resulting in Controls (black), *Foxp1* heterozygous (light blue) and *Foxp1* homozygous (red) mice.

To study the interaction between *Foxp1* and *Foxp2* genes in the striatum and their possible mutual regulation, mice with global heterozygous disruption of Foxp1 and Foxp2 were intercrossed (Figure 2.5). The Foxp2 line carries a premature stop codon close to the human R328X nonsense mutation found in a second family segregating *Foxp2*-related speech and language deficits (*Foxp2-S321X*) (Groszer *et al.* 2008). Foxp1 global heterozygous mice were obtained from the offspring of the Foxp1$^{flox/+}$; Rgs9-Cre x Foxp1$^{flox/flox}$ intercross (Figure 2.4). In rare cases germ line deletion occurred in these animals i.e. they genotyped positive for deletion of the loxP flanked sequence but not for Cre (*Foxp1-Δ11-12*). The offspring resulting from this cross are as follows: mice with wild-type *Foxp1* and *Foxp*2 alleles (abbreviated to Controls), mice heterozygous for *Foxp1-Δ11-12* with wild-type (WT) Foxp2 alleles (abbreviated to Het1), mice heterozygous for *Foxp2-S321X* and with wild-type *Foxp1* alleles (abbreviated to Het2) and mice heterozygous for *Foxp1-Δ11-12* and *Foxp2-S321X* (abbreviated to dHet).

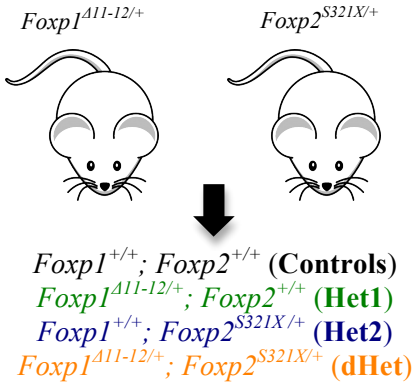

Figure 2.5. Generation of experimental animals to study the interaction between *Foxp1* and *Foxp2* genes in the striatum. Heterozygous mice from *Foxp1-Δ11-12* line were crossed with heterozygous mice from *Foxp2-S321X* line, resulting in Controls (black), Het1 (green), Het2 (dark blue) and dHet (orange) mice.

2.3. Genotyping

2.3.1. DNA extraction

DNA for use in genotyping was extracted from ear punches or tail biopsies, when the first is not possible. Following the DNA extraction kit instructions (*REDExtract-N-Amp™ Tissue PCR Kit, SIGMA-ALDRICH*), 100 microliters (µL) of the extraction solution and 25 µL of the tissue preparation solution were added to each sample and incubated at room temperature (RT) for 10 minutes (min), followed by a 3 min incubation at 95 ºC (*Thermomixer compact, number 5350, Eppendorf*). The final step was the addition of 100 µL of the neutralization solution B, followed by homogenization in a vortex (*VWR International*). The samples were stored at 4 ºC until the genotyping was completed.

2.3.2. PCR amplification

Mice were genotyped using PCR amplification to determine whether the *Foxp1* conditional allele was present and to determine the presence of the Cre gene. To evaluate the interaction between *Foxp1* and *Foxp2* genes, PCR amplification was also performed to genotype mice from *Foxp1-Δ11-12* and *Foxp2-S321X* lines.

The PCR reagents were added in accordance to the PCR kit instructions (*REDExtract-N-Amp™ Tissue PCR Reaction Mix, SIGMA-ALDRICH*) (Table 2.1).

Table 2.1. Quantities of PCR reagents added in each reaction tube. *x* represents the volume of water added to make up to 20 µL of total volume. *y* represents the volume of each primer (forward and reverse) added to maintain a concentration of 0,4 micromolar (µM) in the reaction. Adapted to REDExtract-N-Amp™ Tissue PCR Kit Protocol (*SIGMA-ALDRICH).*

Reagent	Volume (µL)
Water	*x*
REDExtract-N-Amp PCR Reaction Mix	10
Forward Primer 0,5 µM	*y*
Reverse Primer 0,5 µM	*y*
Tissue Extract	4
Total volume	20

Specific primer combinations were used for each PCR reaction. The *Foxp1* PCR reaction was used to investigate the presence/absence of *Foxp1* conditional allele. Cre1 and Cre2 PCR reactions were performed to conclude about the presence/absence of the Cre recombinase gene. *Foxp1-Δ11-12*

reaction was used to detect the deletion of the neo marker from the mouse germline in order to generate mice with a germline *Foxp1* mutation. *Foxp2-S321X* reaction was performed to evaluate the presence of the mutation resulting in the premature *Foxp2* stop codon (Table 2.2).

Table 2.2. Specific primer combinations used for mice genotyping. *Foxp1cKO1* and *Foxp1cKO2* were used for the *Foxp1* PCR reaction. *Cre-F*, *Cre-R*, *MT3-F* and *MT3-R* were used for the *Cre1* PCR reaction. *Cre-3* and *Cre-4* were used for the *Cre2* PCR reaction. *CK01* and *10R* were used for the *Foxp1-Δ11-12* PCR reaction. *7F* and *7R* were used to perform the *Foxp2-S321X* PCR reaction. All primers were purchased from *SIGMA-ALDRICH*.

PCR reaction	Primers	Nucleotide sequence
Foxp1	***Foxp1cKO1***	5'- CTC CTA GTC ACC TTC CCC AGT GC -3'
	Foxp1cKO2	5'- GAA CAC TGT CGA ATG ACC CTG C-3'
Cre1	***Cre-F***	5'- GGT TTC CCG CAG AAC CTG AA -3'
	Cre-R	5'- AGC CTG TTT TGC ACG TTC ACC -3'
	MT3-F	5'- CCT AGC ACC CAC CCA AAG AGC TG -3'
	MT3-R	5'- GGT CCT CAC TGG CAG CAG CTG CA -3'
Cre2	***Cre-3***	5'- CAC TCA TGG AAA ATA GCG ATC-3'
	Cre-4	5'- ATC TCC GGT ATT GAA ACT CCA GCG C -3'
Foxp1-Δ11-12	***CK01***	5' - CTC CTA GTC ACC TTC CCC AGT GC - 3'
	10R	5' - CAC CCT CTC CAA GTC TGC CTC AG - 3'
Foxp2-S321X	***7F***	5' – ATA GTA TGG AAG ACA ACG GCA TC - 3'
	7R	5' – GAT GGG GTT AGT GAA TGT TCT CA - 3'

The PCR reaction tubes were gently mixed. The final step was the PCR amplification reaction in a thermocycler (*C-1000 Touch Thermal Cycler, CFX96 Real-Time System, Bio-Rad*), using the optimised amplification parameters shown bellow (Tables 2.3 to 2.5).

Table 2.3. Optimised amplification parameters of PCR reaction *Foxp1*. T represents the temperature of the PCR step in ºC. s represents the time in seconds.

PCR step	PCR reaction ***Foxp1***		
	T (ºC)	Time	Cycles
Initial denaturation	95	15 min	1
Denaturation	95	30 s	
Annealing	65 to 58 (touchdown 0,5/cycle)	30 s	13
Extension	72	45 s	
Denaturation	95	30 s	
Annealing	58	30 s	25
Extension	72	40 s	
Final extension	72	7 min	1
Holding	4	-	-

Table 2.4. Optimised amplification parameters of PCR reactions Cre1 and Cre2. T represents the temperature of the PCR step in ºC.

PCR step	PCR reactions					
	Cre1			**Cre2**		
	T (ºC)	Time	Cycles	T (ºC)	Time	Cycles
Initial denaturation	94	3 min	1	94	2 min	1
Denaturation	94	30 s		94	45 s	
Annealing	58	30 s	35	60	1 min	35
Extension	72	30 s		72	90 s	
Final extension	72	5 min	1	72	8 min	1
Holding	4	-	-	4	-	-

Table 2.5. Optimised amplification parameters of PCR reactions *Foxp1-Δ11-12* and *Foxp2-S321X*. T represents the temperature of the PCR step in ºC.

PCR step	PCR reactions ***Foxp1-Δ11-12*** ***Foxp2-S321X***		
	T (ºC)	Time	Cycles
Initial denaturation	95	15 min	1
Denaturation	94	1 min	
Annealing	55	1 min	35
Extension	72	1 min	
Final extension	72	10 min	1
Holding	4	-	-

2.3.2.1. Restriction enzyme digest

The mutation in the *Foxp2-S321X* line results in the formation of an AflII restriction enzyme site, which is utilised for genotyping (Figure 2.6). A restriction enzyme digestion with AflII (*cat. R0520S, New England BioLabs*) was performed as shown in Table 2.6.

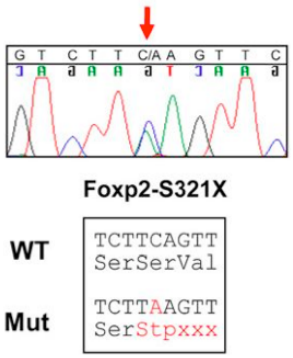

Figure 2.6. Sequence traces showing each heterozygous mutation with corresponding changes in coding sequence (Groszer *et al.* 2008).

Table 2.6. Quantities of restriction enzyme digest. Quantities of reagents added in each reaction tube (*cat. R0520S, New England BioLabs*).

Reagent	Volume (µL)
Water	6,45
AflII	0,25
BSA	0,3
10X CutSmart buffer	3
PCR product	20
Total volume	30

The restriction enzyme digestion tubes were gently mixed. The final step was the incubation in a thermocycler (*C-1000 Touch Thermal Cycler, CFX96 Real-Time System, Bio-Rad*) for 3 h at 37 ºC.

2.3.3. Gel electrophoresis

Agarose gels were used to separate DNA fragments of different sizes in PCR samples. Gels with specific concentrations of agarose (*ThermoFisher Scientific*) for each PCR protocol (Tables 2.3 and 2.4) were made in 1% Tris-acetate-EDTA (TAE) (*Sigma-Aldrich*) running buffer. 3,5 µL/50 millilitres (mL) of loading dye (*DNA Gel Loading Dye, ThermoFisher Scientific*) was added to facilitate the visualisation of the gel bands. A 100 base pairs (bp) ladder (*Precision molecular mass standard, Bio-Rad*) was used to determine the size of the bands. The gel was run at ≈ 140 Volts (V) for 50 min and viewed under ultraviolet light (UV) in a transilluminator *(ChemiDoc™ MP System, Bio-Rad)*. The genotype of the animals could then be determined, according to the expected size of the bands (Table 2.6).

Table 2.7. Expected sizes of the genomic fragments. Expected sizes, in bp, of the genomic fragments for each region, which allows the mice genotyping (Feng *et al.* 2010; Dang *et al.* 2006; Groszer *et al.* 2008).

PCR reaction	Fragment	Size (bp)
Foxp1	WT	280
	Conditional	370
Cre1	WT	300
	Cre	150
Cre2	Cre	500
Foxp1-Δ11-12	WT	1200
	Mutant	450
Foxp2-S321X	WT	468
	Mutant	135 and 332

2.4. Perfusion and dissection

For histology, all of the blood from the brain was removed, since it would interfere with the staining and the correct visualization of the brain cells. The perfusion and dissection were performed as previously described (Gage *et al.* 2013).

Beforehand, the apparatus and solutions for the perfusion, a peristaltic pump *(Flex-Pro A2 Peristaltic Metering Pump, Blue-White),* phosphate-buffered saline (PBS) (*Glasswash and Media Preparation Platform, Champalimaud Foundation*) and fixative paraformaldehyde 4 % (PFA) (*Glasswash and*

Media Preparation Platform, Champalimaud Foundation) were prepared and assembled as shown bellow (Figure 2.5).

Mice were weighed and lightly anesthetized with cotton soaked with isoflurane (*JD Medical*) and then deeply anesthetized with an intraperitoneal injection of ketamine/xylazine mixture: 12 % body weight ketamine (*Imagene*) and 8 % body weight xylazine *(Rompun xylazine 100 milligrams (mg)/mL Injectable, Bayer DVM)* (0,01 mL per g of body weight). The perfusion technique consisted of opening the abdomen, cutting through the peritoneum and carefully separating the liver from the diaphragm. To reach the heart, the diaphragm was cut to expose the pleural cavity and the sternum clamped and placed over the head. Then the perfusion needle connected with the peristaltic pump was inserted on the left ventricle into the ascending aorta and a small incision was made on the right atrium (Figure 2.4).

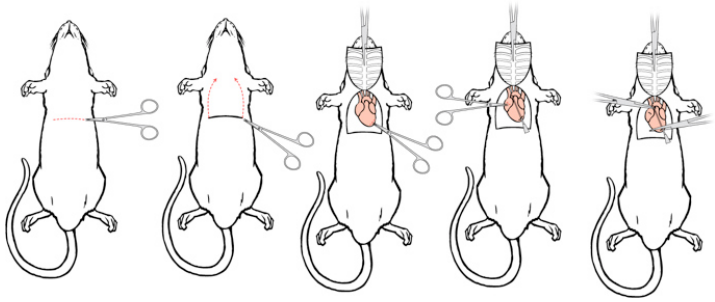

Figure 2.7. The major steps of mice perfusion.

This allowed the PBS to replace the blood all over the animals' body, and the blood to exit through the right atrium. After approximately 15 to 20 min, all the blood was replaced by the buffer (PBS) and then by the fixative (PFA).

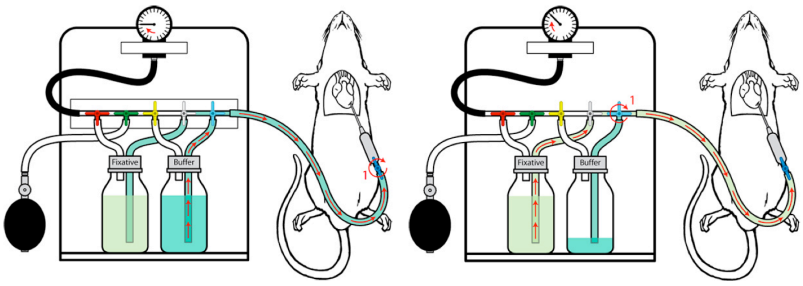

Figure 2.8. Schematic diagram showing the perfusion steps.

After the perfusion step, the brain was carefully removed from the head. A midline incision from the neck to the nose was made and the skull was exposed. Carefully, the skull was removed and the brain was exposed (Figure 2.6).

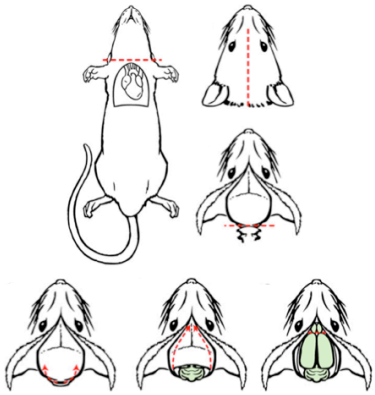

Figure 2.9. The major steps of brain dissection.

The brain was stored in PFA for at least 24 h before being sectioned and then embed in PBS.

2.5. Brain sectioning

After incubation in PFA, the brain was sectioned using a vibratome (*VT 1000 S, Leica*). The apparatus was prepared in accordance with machine instructions. The brain was embedding in agarose 2,4 % to facilitate the sectioning. Sections were floated off the specimen in PBS and placed in multiwell plates and then stored at 4 ºC until histological procedures.

2.6. Immunohistochemistry

Sections were washed for 3 x 5 min in phosphate-buffered saline (PBS) (*Glasswash and Media Preparation Platform, Champalimaud Foundation*) and placed in 3 % hydrogen peroxide (H_2O_2) (*Glasswash and Media Preparation Platform, Champalimaud Foundation*) for 10 min to quench endogenous peroxidases. Following 3 x 5 min washes in PBS sections were put in blocking solution (5% heat inactivated horse serum (*New Zealand Origin, catalog number 26050070, Gibco*), 2 % Bovine Serum Albumin (*Lot #SLBL2871V, Sigma-Aldrich*) and 0,2 % Triton-X 100 (*Lot #110M00093V, Sigma*)) for 45 min. Subsequently the sections were incubated overnight (ON) at room temperature (RT) in primary antibody, rabbit monoclonal antibody to FOXP1 (*ab134055, [EPR4113], Lot GR97096-11, abcam*) 1:200 in blocking solution. The following day, sections were washed 3 x 5 min in PBS before incubating in secondary antibody, biotin-conjugated donkey anti-rabbit IgG (*Lot 86689, Jackson ImmunoResearch*) 1:500 for 2 h at RT. Then sections were washed 3 x 5 min in PBS before incubating in Vectastain ABC KIT Standard (*Elite ABC, Vector Laboratories*) for 30 min at RT. The sections were washed 3 x 5 min in PBS before the incubation in peroxidase substrate ImmPACT DAB (3,3-diaminobenzidine substrate) (*Vector Laboratories*) for 7 min, after which the reaction was immediately stopped with tap water. Sections were mounted onto slides (*Superfrost Plus, Thermo Scientific*) and left to dry ON. They were then washed in tap water for 2 min and dehydrated through a molecular grade ethanol (*Lot 1201930, Fisher Chemical*) series for 2 min at each concentration (50 %, 70 %, 90 %, 100 % and 100 %). Then the sections were washed in histological clearing agent Histo-Clear (*Lot 04-12-31, national diagnostics*) and mounted with histological mounting medium Histomount (*Lot 03-08-20, national diagnostics*) with coverslips (*Thermo Scientific*).

The brain sectionss were imaged on a Widefield Fluorescence Scanning Microscope (*Axio Imager M2, Zeiss*) and analysed with AxioVision Microscopy Software (*Version 4.8.2, Zeiss*) with Image Processing and Analysis in JAVA (ImageJ).

2.7. Western blot

2.7.1. Protein extraction

Tissues from the striatal and cortex regions of *Foxp1* homozygous and Control mice was dissected into lysis RIPA buffer (*Lot #SLBL7395V, Sigma-Aldrich*), 0,5 mL for 50 mg of sample, after the addition of phosphatase inhibitor (*PhosSTOP EASYpack, reference 04906837001, Roche*) and protease inhibitor (*cOmplete Tablet, Mini EDTA-free EASYpack, reference 04693159001, Roche*), in a proportion of 1 tablet of each for 10 mL of RIPA buffer. Then, the tissues were disrupted by homogenisation (Potter-Elvehjem, *RW16 basic, IKA*) and subsequently by sonication (*Vibra Cell sonicator, model 75185, Bioblock Scientific*) at 30 % of amplitude for approximately 30 s. Lysates were centrifuged at 10000 relative centrifugal force (G) for 10 min.

2.7.2. Protein quantification

The protein concentrations of the supernatants were determined by Pierce BCA Protein Assay (*Lot #NE173647, Thermo Scientific*) in accordance with kit instructions. The working reagent was prepared by the addition of reagent A to reagent B in a proportion of 50:1. Standards and samples were added to microplates in triplicate, with a protein sample to working reagent ratio of 1:8. The samples were incubated at 37 ºC for 30 min and then moved to RT for 5 min. The quantification was performed in the spectrophotometer NanoDrop (*model 2000/2000c, Thermo Scientific*). The values obtained were used to determine the standard curve and then the protein concentration of each sample.

2.7.3. Gel electrophoresis

The loading buffer for gel electrophoresis was prepared with Laemmli sample buffer (*cat. #1610737, Bio-Rad*) and 2-Mercaptoethanol (*cat. #1610710, Bio-Rad*) with a ratio of 10:1. A sample volume equivalent to 30 µg of protein was added to the loading buffer. Samples were then heated at 100 ºC for 10 min and centrifuged for 30 s. The protein samples were ran on commercial gels (*Mini-PROTEAN® TGX™ Precast Gels, 4-15 %, Bio-Rad*). To preparing the cassette, the comb was removed by pulling upward and the tape was also removed from the bottom of the cassette, according to the Mini-PROTEAN® TGX™ Precast Gel Quick Start Guide (Rev C, document number 10026447, Bio-Rad). To assemble the Mini-PROTEAN Tetra Cell (Bio-Rad), the running buffer was added to the inner and outer chambers and the wells were cleaned. The samples and the Precision Plus Protein™ WesternC™ standards (Bio-Rad) were load into the wells in a total volume of 15 µL per well.

2.7.4. Semi-dry transfer

To perform the electrophoretic protein transfer, a semi-dry transfer method was used. The transfer buffer (500 mL per transfer) was prepared with 100 mL of methanol, 100 mL of transfer buffer 5x (60,6 gramme (g) Trizma base (*Sigma-Aldrich)*, 288 g Glycine (*Calbiochem*) and deionized water up to 4 L) and 300 mL of deionized water. The membrane was soaked in methanol for 5 min and then into the transfer buffer previously prepared. The "sandwich" assembly was constructed according to the kit instructions (Figure 2.7). The transfer occurred at 12 V for 1 h. To check if the proteins had correctly transferred from the gel to the membrane, the latter was soaked in 5 mL of Ponceau stain. To remove the staining the membrane was washed 3 x 5 min in a mixture of tris-buffered saline (TBS) and Polysorbate 20 (Tween 20) (TBST).

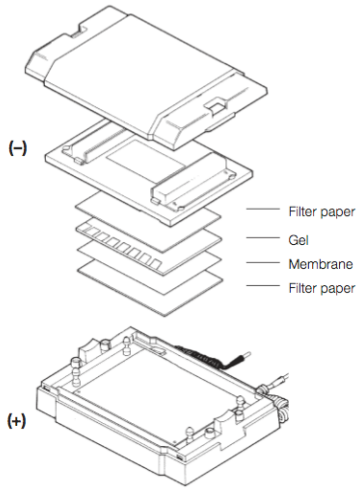

Figure 2.10. Assembly of the Trans-Blot SD semi-dry cell.

2.7.5. Antibody probing

The blocking solution was prepared with 5% of Blot-Grade Blocker in a mixture of TBST. The membranes were incubated in blocking solution for 1 h at RT. The primary antibody incubation was done with primary antibody rabbit monoclonal antibody to FOXP1 (*ab134055, [EPR4113], lot no. GR97096-11, abcam*) 1:200 in blocking solution and primary antibody monoclonal anti-β-actin (produced in mouse, monoclonal AC-15, product number A5441, lot no. 121M4846, *Sigma-Aldrich*) 1:100000 in blocking solution. The membrane was washed 3 x 15 min in TBST before the secondary incubation for 1 h at RT in the respective secondary antibody: donkey anti-rabbit conjugated horseradish peroxidase (HRP) for Foxp1 1:2000 in blocking solution and goat anti-mouse conjugated HRP for β-actin 1:2000 in blocking solution. The membrane was washed 3 x 15 min in TBST and then was cut between the bands 50 kilodalton (kD) and 75 kD. Foxp1 band is expected have a size of 75 kD and β-actin a size of 42 kD.

2.7.6. Detection

The detection solutions Amersham™ ECL™ Prime Western Blot Detection Reagent (GE Healthcare) were left at RT for 20 min to equilibrate before the incubation. The reagents A and B, iluminol and peroxide, were mixed in a ratio of 1:1 to a working solution, with a final volume of detection reagent of 0,1 mL/centimeter^2 (cm^2) membrane. The Foxp1 and *β*-actin membranes were incubated with detection reagent during specific periods for each condition (Table 2.7).

Table 2.8. Time of incubation. Time of incubation in Amersham™ ECL™ Prime Western Blot Detection Reagent (GE Healthcare).

	Foxp1 membrane	***β*-actin membrane**
Cortex	5 min	30 s
Striatum		10 s

After the incubation with the detection reagent, membranes were rinsed in deionised water and placed on a plastic sheet. Following the detection on the imaging apparatus Amersham™ Imager 600 (GE Healthcare) with the times described in Table 2.8.

Table 2.9. Time of exposure. Time of exposure in the imaging apparatus Amersham™ Imager 600 (GE Healthcare).

	Foxp1 membrane	***β*-actin membrane**
Cortex	72 min	15 s
Striatum	10 min	1 s

2.7.7. Data analysis

The protein detection images, namely the density of bands on western blot were analysed with ImageJ, in accordance with Luke Miller's protocol (Miller 2010).

The images were opened in the software (File > Open) and converted to grayscale (Image > Type > 8-bit). Rectangular selections (Rectangular Selection from the ImageJ toolbar) were drawn around each lane or well. To identify each lane, a number was assigned (Analyse > Gels > Select First Lane or Select Next Lane). This step was followed by the creation of a profile plot of each lane (Analyse > Gels > Plot Lanes), which represents the relative density of the contents of the rectangle over each lane, from top to bottom. As images of real western blots will always have some background, it was necessary to close off the peak so that the size could be measured (Straight Line selection from the ImageJ toolbar). Subsequently the highlighted peaks (Wand tool from the ImageJ toolbar) and the respective sizes (Analyse > Gels > Label Peaks), expressed as a percentage of the total size of all of the highlighted peaks, using a peak as a standard. The calculation of the relative density was done by dividing the percentage value of each lane by the percentage value of the standard.

2.8. Accelerating rotarod

The rotarod test was used to provide an overall assessment of motor coordination, balance and evaluation of motor-skill learning of adult mice.

A computer-interfaced rotarod (ENV-577MAX, Med Associates Inc., Georgia, Vermont, United States of America) was set to accelerate from 6 to 60 revolutions per minute (rpm) over a 300 s time period. Mice (with more than 10 weeks or 2 months of age) were trained for 5 consecutive days with 1 daily session consisting of 10 trials separated by 300 s resting periods. Mice were placed forward on the rotarod and trials were deemed to have started when the rod began to turn. Trials ended when mice fell from the rod or after 300 s elapsed. If the mouse immediately fell off at the beginning of the first trial, that trial was not considered and the mouse performed a new trial. At the end of each trail, the apparatus was sprayed with ethanol 70 % and wiped clean with paper towels.

Learning rate was calculated as follows:

$$\frac{\text{mean latency to fall}_{\text{trials 9 and 10}} - \text{mean latency to fall}_{\text{trials 1 and 2}}}{9} \quad (2.1)$$

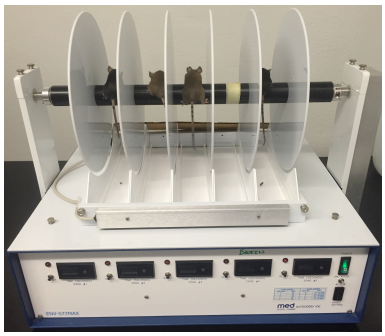

Figure 2.11. Mice performing the accelerating rotarod task.

2.9. Operant motor-sequence learning task

The operant motor-sequence learning task is used to investigate the learning and performance of novel motor-sequences of adult mice (around 13 weeks or 3 months of age).

Before the first day of training mice were submitted to 48 h of food restriction and 12 h of water deprivation, and were then maintained at around 85 % of their original body weight for the duration of the task. Mice were habituated in operant chambers housed in sound attenuating boxes (Med-Associates, St. Albans) as previously described (Jin *et al.* 2010).

Figure 2.12. Operant chambers. A lever was extended to the left of a food magazine containing a metal cup into which 10% sucrose solution was delivered from a syringe pump.

For habituation, animals were placed into the chambers for 30 min of exploration. The day after, the lever was extended and a reinforcement was delivered after each press. The possible number of reinforces earned increased each day (5, 15, 30). A session was completed after the number of reinforcements had been delivered or 90 min passed. As soon as mice got the thirty reinforcements in 90 min, the acquisition period ended and the main part of the task began. Mice get a sucrose reinforcement after eight lever presses (fixed-ratio 8 schedule, FR8). Initially pressing is self-paced, but after twelve days of training (also called self-paced FR8 period) a time constraint is added and the eight presses must be completed at increasingly high speeds (first day - 8 presses in 16 s, second day - 8 presses in 12 s, subsequent days - 8 presses in 8 s, 6 s, 4 s and 2 s) (also known as high-speed FR8 period) (Figure 2.10). The task takes approximately 30 consecutive days to complete and allows detailed analyses of the microstructure of lever-pressing behaviour.

Data recorded included the number of lever presses, the syringe pump activations, head entries into the food magazine (detected by infrared beam) and the number of licks in the cup (detected by contact lickometer).

Figure 2.13. Operant motor-sequence learning task timeline. The experience starts with an acquisition period. Follow the self-paced FR8 and it ends with a high-speed FR8 period.

2.10. Sociability and social preference for social novelty task

Sociability and preference for social novelty were tested in adult mice (around 22 weeks or 5 months of age) using a rectangular three-chamber box (each chamber 300 x 150 x 150 mm) with a door (50 x 50 mm) in each delimiting wall, which allows free access to each chamber (Figure 2.11). This task is divided into two different phases: the first is to investigate social interaction or the tendency to spend time with another conspecific and the second is to visualise the preference for social novelty or the ability to discriminate and choose between familiar and new conspecifics (Yang *et al.* 2011; Moy *et al.* 2007).The test mouse was placed in the centre chamber with doors opened during 10 min for habituation and exploration of the compartments and the empty cups. To give a choice between spending time in the side containing an unfamiliar or stranger conspecific mouse (C57BL/6J mouse of

the same gender as the test mouse without previous physical contact with the test mouse) or remaining alone, a stranger mouse was placed in a cup for 5 min, to allow visual, auditory, olfactory and tactile stimuli (social interaction). In the second phase of the task, a second unfamiliar or specific stranger conspecific mouse was placed in a cup in the other side for 5 min (preference for social novelty). The location for the first stranger was alternated between the left and right sides of the social test box across subjects. The task was video taped for each mouse.

Figure 2.14. Three-chamber apparatus.

2.11. Analyses and statistics

Graphs and statistical analyses were done with GraphPad Prism software. Data were analysed using two-way analysis of variance (ANOVA) or two-way repeated measures ANOVA followed by Dunnett's post hoc tests where appropriate. Lever-press data was analysed using Custom written Matlab code (Mathworks, Natick, MA, USA). Videos from the social interaction and preference for social novelty test were analysed using the video tracking system ANY-maze (San Diego Instruments, San Diego, USA). Close interaction behaviour was also scored manually.

3. Results

3.1. Generation of mice with striatal-specific disruption of *Foxp1*

Foxp1, a gene linked with ASDs, is expressed in the cortex, hippocampus, thalamus and striatum of the mouse brain. To determine the functions of *Foxp1* in the striatum, the brain region involved in action related to habitual learning and goal-directed learning, a transgenic mouse line was created. $Foxp1^{flox/flox}$ mice were crossed with $Rgs9\text{-}Cre^{+}$ mice to generate mice with *Foxp1* disrupted specifically in the striatum. In order to obtain transgenic mice with *Foxp1* specifically deleted in the striatum in homozygosity and heterozygosity, *Foxp1* heterozygous mice from the previous breeding were selected and crossed with $Foxp1^{flox/flox}$ mice (see Materials and Methods 2.2 for details). The PCR reaction *Foxp1* was used to detect the presence of *Foxp1* conditional alleles. To detect the success of the disruption of the *Foxp1* gene mediated by Cre recombinase, the PCR reactions *Cre1* and *Cre2* were performed (Figure 3.1).

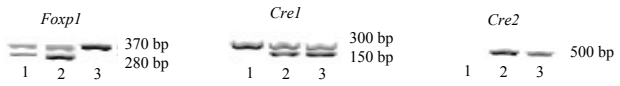

Figure 3.1. Example PCR analysis of experimental animals using *Foxp1*, *Cre1* and *Cre2* reactions. Shown is a PCR result indicating the presence of the WT *Foxp1* allele (280 bp) in animals 1 and 2, and the conditional *Foxp1* allele in animals 1,2 and 3 (370 bp). The gel also shows the presence of the *Cre* recombinase gene for animals 2 and 3 (*Cre* has 150 bp and 500 bp for *Cre1* and *Cre2* PCR reactions respectively). Animals with different genotypes are identified with "1", "2" or "3".

For the *Foxp1* PCR reaction, the expected sizes of the DNA fragments are 280 bp and 370 bp for WT and conditional fragments respectively (Table 2.7). Animal 3 revealed only a dense band with 370 bp and animals 1 and 2 showed WT and conditional fragments. The analysis of *Foxp1* PCR reaction identified animals 1 and 2 as heterozygous and animal 3 as homozygous for *Foxp1* conditional allele.
The *Cre1* PCR reaction expected sizes of the DNA fragments are 300 bp and 150 bp for WT and Cre fragments respectively (Table 2.7). Animals 2 and 3 had two fragments with approximately 150 bp and 300 bp, the presence of smaller fragment (150 bp) indicates the presence of Cre.
The *Cre2* PCR reaction was done to confirm the *Cre1* PCR reaction result. The expected size for Cre fragment is 500 bp (Table 2.7). The PCR analysis for animal 1 does not show any Cre fragment, as opposed to animals 2 and 3, who have a single fragment with 500 bp, indicating the presence of the Cre.
In accordance with the PCR analysis, animal 1 ($Foxp1^{flox/+}$; $Rgs9\text{-}Cre^{-}$; heterozygous for the *Foxp1* allele; absence of the Cre) is a Control, animal 2 ($Foxp1^{flox/+}$; $Rgs9\text{-}Cre^{+}$; heterozygous for the *Foxp1* allele; presence of the Cre) is a *Foxp1* heterozygous and animal 3 ($Foxp1^{flox/flox}$; $Rgs9\text{-}Cre^{+}$; homozygous for the *Foxp1* allele; presence of the Cre) is a *Foxp1* homozygous.

3.2. Foxp1 protein expression in mice with striatal-specific *Foxp1* disruption

Extracts from the striatal and cortex regions were analysed by western blot using a monoclonal primary antibody to Foxp1 and a primary antibody to β-actin housekeeping protein, to determine the impact of Cre-mediated deletion at the protein level. In order to compare the protein expression levels between several samples from different genotypes (Controls and *Foxp1* homozygous) on the same blot, the housekeeping protein β-actin was used to normalise the data (Figure 3.2).

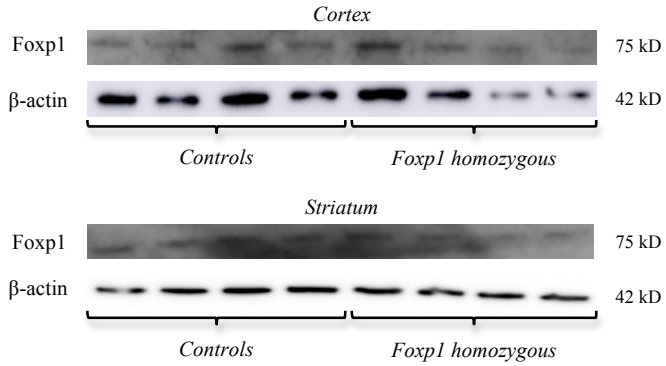

Figure 3.2. Western blot. Western blot analysis of Foxp1 in cortex and striatum regions of Controls (n=4) and *Foxp1* homozygous (n=4) mice. The expected sizes for Foxp1 and β-actin proteins are 75 kD and 42 kD respectively.

A single band corresponding to full-length Foxp1 was observed in Controls (a number of other bands were also visible which in some cases corresponded to predicted Foxp1 isoforms and in other cases were non-specific). Unexpectedly, this band was also present in *Foxp1* homozygous extracts at similar levels to what was observed in Controls.

The protein bands were analysed with ImageJ, in accordance with Luke Miller's protocol (Miller 2010), to compare the relative density of bands quantitatively (Figure 3.3). This analysis supported out initial observations but was problematic because of the high levels of background present on the Foxp1 blots, caused by the long exposure times needed to visualise bands. The Foxp1 antibody had to be used at a high concentrations (1:200) and did not appear to recognise the epitope well under the denaturing conditions found in western blot.

This data suggests that Foxp1 was not deleted in mice with striatal-specific disruption of *Foxp1*. Nevertheless, due to the technical difficulties encountered with the western blot a immunohistochemistry was also performed.

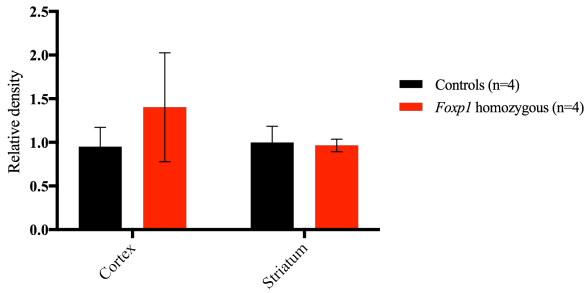

Figure 3.3. Relative density. Relative density of protein in Foxp1 and β-actin protein bands in cortex and striatum regions of Controls (n=4) and *Foxp1* homozygous (n=4) mice. n represents the number of subjects in each condition. Data shown are represented as mean ± standard error of the mean (SEM).

3.3. Histological validation shows striatal-specific *Foxp1* knockdown rather than knockout in *Foxp1* homozygous mice

For the histological validation of mice with striatal-specific *Foxp1* disruption, immunohistochemistry was performed using a monoclonal primary antibody to Foxp1 (Figure 3.4). In immunohistochemistry conditions, where proteins retain their native configuration, the Foxp1 antibody worked efficiently and specifically.

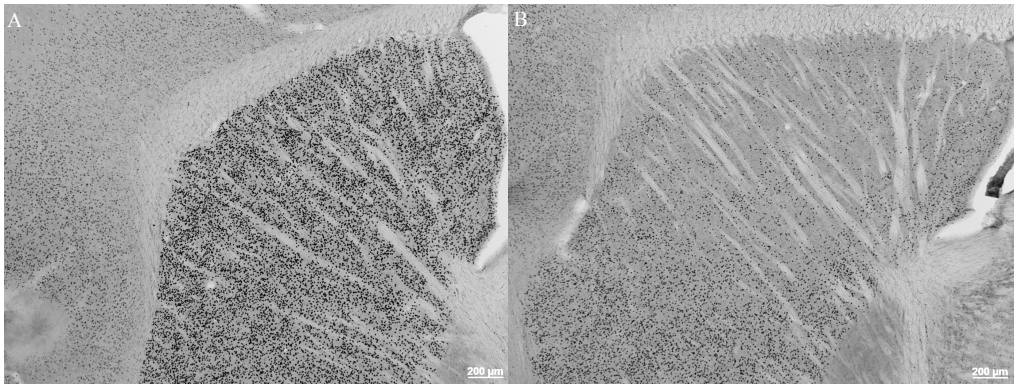

Figure 3.4. Immunohistochemistry. Representative images of immunohistochemistry of cortex and striatum of Controls (A) and *Foxp1* homozygous (B) with a magnification of 20 x.

Foxp1 loss was substantial in the dorsal striatum and appreciable in the ventral striatum of *Foxp1* homozygous mice compared to Controls. Similar results were seen in 3 *Foxp1* homozygous and 3 Control brains and sections from each genotype underwent DAB development for equal amounts of time. In general, deletion was not complete in the striatum of *Foxp1* homozygous mice and this line therefore represents a striatal-specific knockdown rather than a striatal-specific knockout.

3.4. Mice with selective *Foxp1* disruption in the striatum are viable and show normal development

Considering equal feeding and maternal care, mouse pups body weight was measured at postnatal days 6, 8, 10, 12, 15, 18 and 21 from *Foxp1* homozygous, *Foxp1* heterozygous and Controls (Figure 3.5).

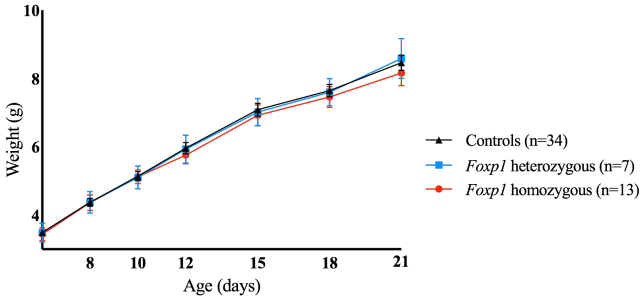

Figure 3.5. Weight development. Weight development of Controls (n=34), *Foxp1* heterozygous (n=7) and *Foxp1* homozygous (n=13) between postnatal days 6 and 21. Data shown are represented as mean ± SEM.

Homozygous and heterozygous conditional knockdown mice appeared normal and increased their weight at the same rate as control littermates (effect of genotype $F_{1,2} = 0.10$, $p > 0.05$) (Figure 3.5). These data indicating that *Foxp1* knockdown in the striatum does not grossly affect mouse development.

3.5. Striatal-specific *Foxp1* knockdown mice do not show gross motor impairment

Experimental mice were tested on the accelerating rotarod to investigate motor-skill learning. Mice were trained for 5 consecutive days, with one daily session of 10 trials spaced by 300 s of interval, with an acceleration rate of 6 – 60 rpm (Figure 3.6).

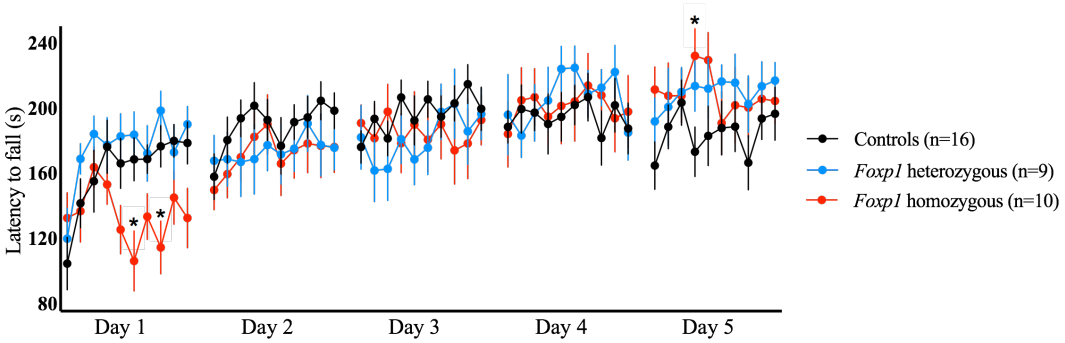

Figure 3.6. Latency to fall. Latency to fall of Controls (n=16), *Foxp1* heterozygous (n=9) and *Foxp1* homozygous (n=10) mice during training on the accelerating rotarod. Data shown are represented as mean ± SEM. $^{*}p < 0.05$.

Learning was evident in all genotypes over the course of training (time x genotype interaction $F_{98, 1568} = 1.53$, $p < 0.05$). However, *Foxp1* homozygous mice showed a reduced latency to fall during the latter part of day 1 compared to Controls, which was significantly different on trials 6 and 8. The learning rate was also significantly reduced in *Foxp1* homozygous mice on day 1 (calculated by comparing performance on the first and last days of training, see Materials and Methods) (Figure 3.7). This deficit is somewhat unusual in that is very transient and would need to be verified in a second cohort of animals. However, careful examination of the data showed that it cannot be attributed to the poor performance of one or two animals in the cohort.

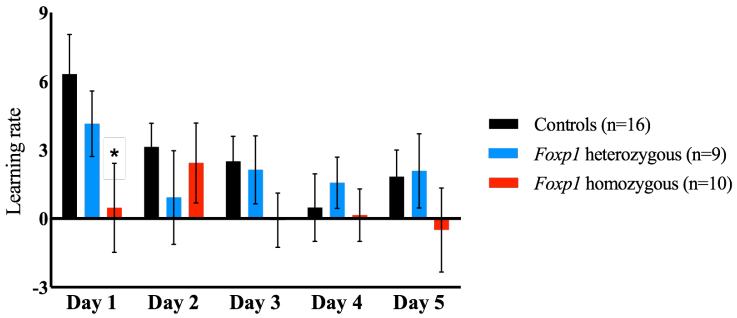

Figure 3.7. Learning rate. Rate of learning in Controls (n=16), *Foxp1* heterozygous (n=9) and *Foxp1* homozygous (n=10) mice during training on the accelerating rotarod. Data shown are represented as mean ± SEM. $^{*}p < 0.05$.

3.6. Striatal-specific *Foxp1* knockdown mice learn and perform sequences of lever-presses normally

An operant lever-pressing task was used to investigate the learning and performance of novel motor-sequences in striatal-specific *Foxp1* knockdown mice. This task has previously been used to show disrupted learning and performance of motor-sequences in mice with striatal-specific deletion of the NMDA receptor (Jin *et al.* 2010). It was also observed increased or decreased variability of lever-pressing in mice with striatal-specific deletion of *Foxp2* or a mouse model of ASDs respectively (French, C. and Martins, G. unpublished data). In this task mice get sucrose reinforcement after eight lever presses (FR8). Initially pressing is self-paced, but after twelve days of training a time constraint is added and the eight presses must be completed at increasingly high speeds (first day – 8 presses in 16 s, second day – 8 presses in 12 s, subsequent days – 8 presses in 8 s, 6 s, 4 s and 2 s), in accordance with the timeline showed in Figure 2.13. There is no signalling of the correct number of presses or the availability of the sucrose reinforce.

The operant lever-pressing task allows observe the number of lever presses and reinforcements and calculate their respective rates (Figure 3.8).

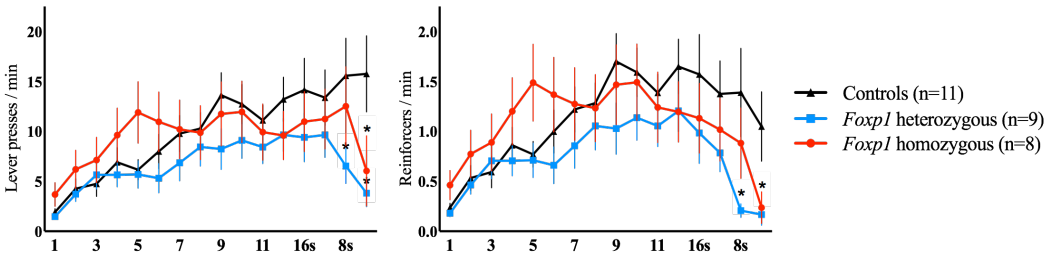

Figure 3.8. Operant lever-pressing. Lever press rate (A) and rate of reinforce delivery (B) of Controls (black) (n=11), *Foxp1* heterozygous (light blue) (n=9) and *Foxp1* homozygous (red) (n=8) through the task. Data shown are represented as mean ± SEM. $^{*}p < 0.05$.

Rates of lever-pressing and reinforce delivery increased during the self-paced phase of training and then decreased in the final days of the high-speed phase when the task became more difficult (LP rate - time x genotype interaction $F_{30, 375} = 2.18$, $p < 0.05$; effect of time $F_{15, 374} = 9.97$, $p < 0.05$: RD rate - time x genotype interaction $F_{30, 375} = 1.92$, $p < 0.05$; effect of time $F_{15, 374} = 11.07$, $p < 0.05$). However, no consistent differences were seen between genotypes (LP rate – effect of genotype $F_{2, 25} = 1.08$, $p > 0.05$: RD rate – effect of genotype $F_{2, 25} = 1.12$, $p > 0.05$) except in the 8 s and 6 s days when rates were reduced in *Foxp1* heterozygous and *Foxp1* homozygous mice (Figure 3.8 A and B). These data suggest that *Foxp1* heterozygous and *Foxp1* homozygous mice are able to learn and perform lever-press sequences.

Concatenation or "chunking" of lever-press sequences has previously been shown to occur in the FR8 task with training, a process which is disrupted when striatal circuits are perturbed (Jin *et al.* 2010). Consistent with these data, pressing in the self-paced training phase became progressively organised into discrete sequences, with the number of presses in a sequence increasing across training in all genotypes (Figure 3.9 A) (effect of time $F_{11, 275} = 15.78$, $p < 0.05$). However, no differences were seen between genotypes in sequence length, sequence duration, inter-sequence interval or within sequence press rate (Figure 9 B-D) (effects of genotype $Fs_{2, 25} \leq 1.14$ 15.78, $ps > 0.05$). Note, one *Foxp1* heterozygous mouse performed very few presses, which skewed the ISI data on day 3. These data indicate that the overall organisation of pressing is intact in *Foxp*1 heterozygous and *Foxp1* homozygous mice and that any deficits would have to be in the timing of pressing.

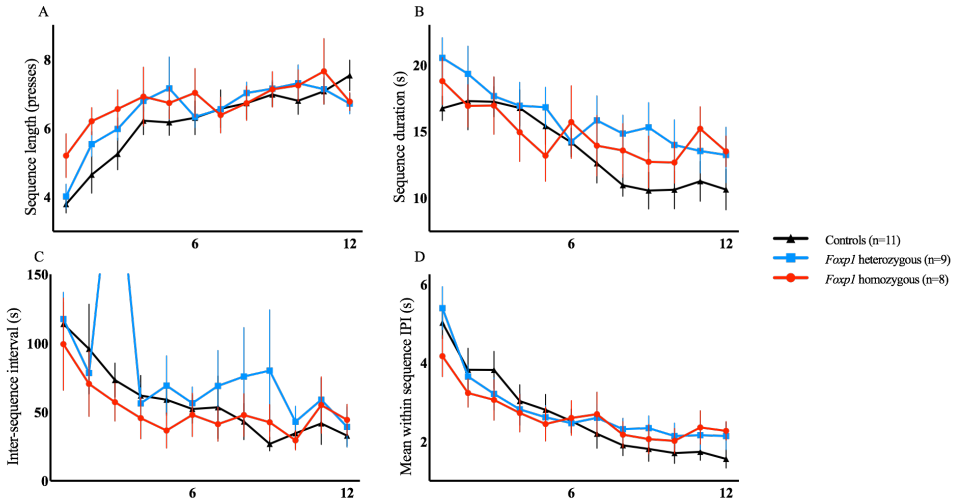

Figure 3.9. Operant lever-pressing. Lever-press sequence analyses during self-paced training sequence. Number of lever presses in a sequence (A), sequence duration (B), inter-sequence interval (C) and mean within-sequence inter-press intervals (IPIs) (D) of Controls (black) (n=11), *Foxp1* heterozygous (light blue) (n=9) and *Foxp1* homozygous (red) (n=8) through the task. Data shown are represented as mean ± SEM.

In order to look in detail at the microstructure of lever-pressing behaviour, inter-press intervals (IPIs) were divided into three types - rapid (no event between presses), check (presses separated by head entry into the food magazine) and consumption (presses separated by head entry and licking). The median and median absolute deviation (MAD) / median (a measure of variability) of these distributions for each of the genotypes were calculated. Again, no differences were observed between striatal-specific *Foxp1* knockdown mice and Controls (Figure 3.10) (effects of genotype $Fs_{2,25} \leq 1.52$ 15.78, $ps > 0.05$), indicating that the learning and performance of fine motor-skills in these animals is normal.

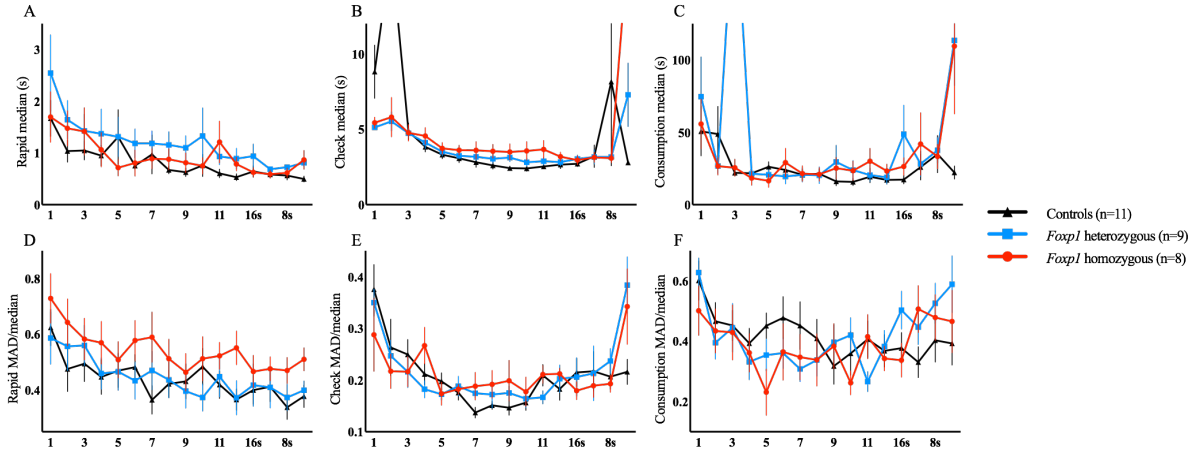

Figure 3.10. Operant lever-pressing. Average median (A-C) and MAD/median (D-F) values of rapid (A and D), check (B and E) and consumption (C and F) IPIs groups of Controls (black) (n=11), *Foxp1* heterozygous (light blue) (n=9) and *Foxp1* homozygous (red) (n=8) through the task. Data shown are represented as mean ± SEM.

3.7. Striatal-specific *Foxp1* knockdown show normal sociability and preference for social novelty

To evaluate social interaction in the striatal-specific *Foxp1* knockdown mice, a 3-chamber task was performed to investigate the sociability and the preference for social novelty (Moy *et al.* 2004). The subjects first had to choose between an unfamiliar mouse and an empty cup, and secondly between the now familiar mouse and a new unfamiliar mouse (see Materials and Methods 2.10 for details).

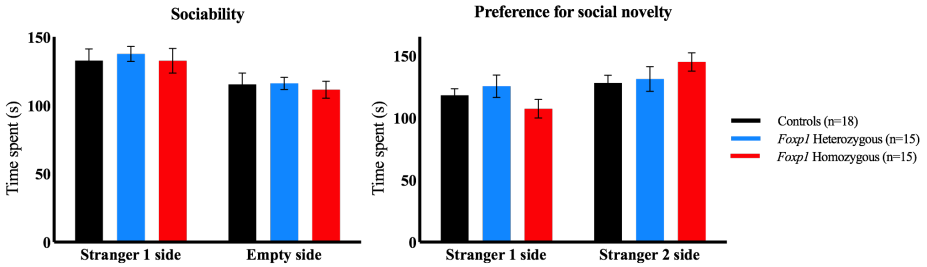

Figure 3.11. Sociability and preference for social novelty. Distribution for duration of time spent in each chamber for the sociability and preference for novelty tests of Controls (black) (n=18), *Foxp1* heterozygous (light blue) (n=15) and *Foxp1* homozygous (red) (n=15).

In the first part of the task, all genotypes preferred the unfamiliar mouse to the empty cup (Figure 3.11 A), suggesting that their sociability is normal. For the second part of the task, *Foxp1* homozygous mice showed a preference for the unfamiliar mouse over the familiar mouse but this preference was less clear in *Foxp1* heterozygous mice and Controls (Figure 3.11 B). Taken together these data suggest that striatal-specific Foxp1 knockdown mice do not have significant deficits in sociability or preference for social novelty.

3.8. Generation of mice heterozygous for *Foxp1* and *Foxp2* globally

Foxp1 disruption in the striatum using the *Rgs9-Cre* line led to a partial knockdown rather than a knockout of the Foxp1 protein, which made some experiments difficult to interpret. Therefore a different strategy was used to investigate *Foxp1* function and potentially cooperative functions with *Foxp2*. Global *Foxp1* heterozygous mice and global *Foxp2* heterozygous mice were crossed to give offspring of four genotypes (Figure 2.5). Considering equal feeding and maternal care, mouse pups body weight was measured at postnatal days 6, 8, 10, 12, 15, 18 and 21 from Controls, Het1, Het2 and dHet mice (Figure 3.12). There was a tendency for dHet pups to show reduced body weight compared to controls (time x genotype interaction $F_{18, 168} = 2.16$, $p < 0.05$; effect of genotype $F_{3, 28} = 2.32$, $p > 0.05$) but this only reached significance on day 21.

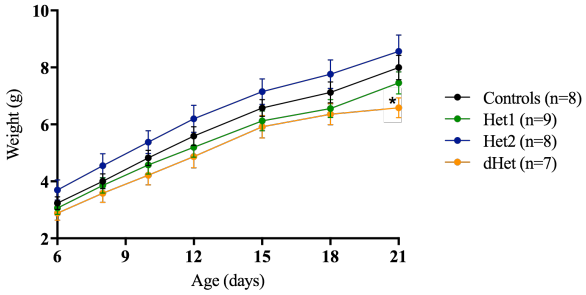

Figure 3.12. Weight development. Weight development of Controls (n=8), Het1 mice (n=9) and Het2 mice (n=8) and dhet mice (n=7) between postnatal days 6 and 21. Data shown are represented as mean ± SEM. $^{*}p < 0.05$.

3.9. Mice heterozygous for *Foxp1* and *Foxp2* show pronounced motor-skill learning deficits

Mice from the *Foxp1* and *Foxp2* heterozygous intercross were also tested with the same conditions as striatal-specific *Foxp1* knockdown mice on the accelerating rotarod to investigate motor-skill learning (Figure 3.13).

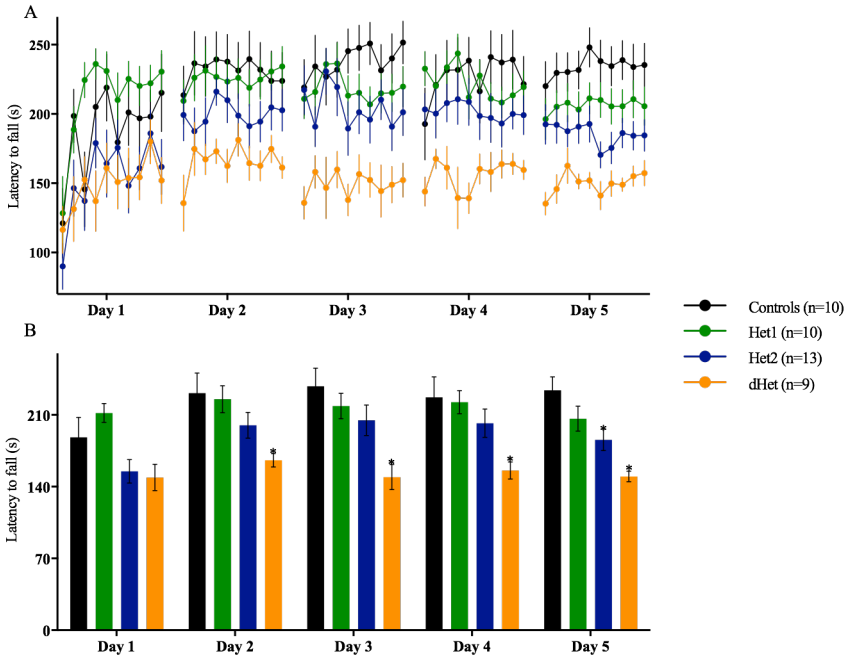

Figure 3.13. Latency to fall. Latency to fall (A) and average of the latency to fall (B) of Controls (n=10), Het1 (n=10), Het2 (n=13) and dHet (n=9) mice during training on the accelerating rotarod. Adult mice with more than 10 weeks or 2 months of age received a training of 10 trials a day for 5 consecutive days. Data shown are represented as mean ± SEM. $^{*}p < 0.05$.

dHet mice fell from the rotarod significantly earlier than Controls on days 2-5 (time x genotype interaction $F_{12, 152} = 2.30$, $p < 0.05$; effect of genotype $F_{3, 38} = 6.37$, $p < 0.05$). Their learning rate also appeared to be perturbed but was not significantly different from that of Controls (Figure 3.14). This was probably due to the big increase in latency to fall seen in Controls on day 2. In addition, Het2 also showed a significantly reduced latency to fall compared to Controls on day 5, which is consistent with previous data (French *et al.* 2012).

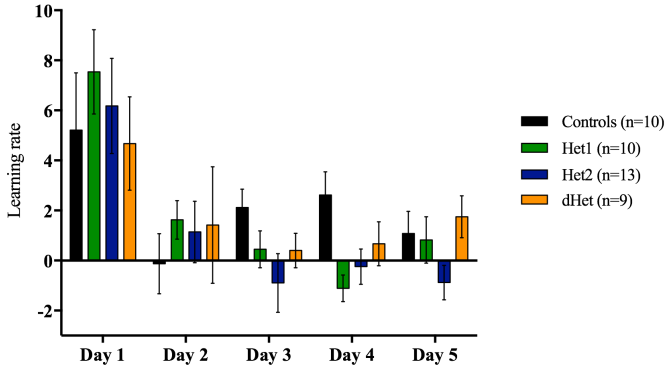

Figure 3.14. Learning rate. Rate of learning in Controls (n=10), Het1 (n=10), Het2 (n=13) and dHet (n=9) mice during training on the accelerating rotarod. Data shown are represented as mean ± SEM.

4. Discussion

It is known that ASDs are linked with the *Foxp1* gene, which is broadly expressed in the striatum, a brain region increasingly being reported to be dysfunctional in ASDs (Fuccillo *et al.* 2016). Therefore a conditional approach was used to selectively knockdown *Foxp1* from striatum, a critical area involved in motor-sequence learning, automatisation of behaviour and social interaction. Homozygous, heterozygous and control subjects for the knockdown of *Foxp1* gene in the striatum were subjected to behavioural tasks to investigate an overall assessment of motor coordination and balance, an evaluation of motor-skill learning, the learning and performance of novel motor-sequences and the sociability and preference for social novelty.

4.1. Level of protein loss in striatal-specific *Foxp1* knockdown mice

Foxp1 protein levels in striatum and cortex (control where *Foxp1* expression was expected) were quantified by western blot techniques. No differences were found between *Foxp1* homozygous mice and Controls in either brain region suggesting that striatal-specific *Foxp1* disruption had not occurred. However the high concentrations of primary Foxp1 antibody used, its specificity, and the long exposure times required to visualise bands continue an issue to pay attention. It was therefore decided to move to a histological approach, where the antibody performed better, and the results are more reliable. Immunohistochemistry showed substantial deletion in dorsal striatum and appreciable deletion in ventral striatum of *Foxp1* homozygous mice, indicating that a knockdown rather than a knockout of *Foxp1* had occurred.

This result was surprising, since the *Rgs9-Cre* line has previously been successfully used to disrupt the NMDA receptor and *Foxp2* in the striatum (Jin *et al.* 2010; French personal communication). It seems that the *Rgs9* promoter does not drive Cre expression in all MSNs and Foxp1 is expressed in the vast majority of these cells, resulting in a partial knockdown. There are two other Cre lines commonly used with conditional mice to generate striatal-specific disruption of genes. The *Dlx5/6-Cre* line was previously crossed with *Foxp2* conditional mice resulting in only modest protein knockdown, probably because Cre in this line in expressed predominantly in interneurons (French personal communication). A further line, *GPR88-Cre,* has also been used to disrupt the NMDA receptor in the striatum and is an option to pursue (Koralek *et al.* 2012). An alternative approach would be to stereotaxically inject Cre-expressing virus into the dorsal or ventral striatum of adult *Foxp1* conditional mice. With this approach Foxp1 protein would be present during development, so results would have to be interpreted accordingly.

4.2. Motor-skill learning and performance are relatively normal in mice with Foxp1 disruptions

Striatal-specific Foxp1 knockdown mice showed normal bodyweight development, although the *Foxp1* gene is crucial in development and differentiation of several organs, and could therefore be used for tasks that assess motor-skill learning and performance. On the accelerating rotarod, *Foxp1* homozygous mice showed a reduced latency to fall compared with Controls in the latter part of day 1. In general, these mice seemed to perform well at the beginning of training but their performance then decreased, before recovering at the start of day 2. This effect was caused by several mice rather than one outlier (the SEM did not increase). This result would need to be confirmed in a second cohort of animals. It should also be noted that there was no difference in latency to fall from the rotarod between global *Foxp1* heterozygous animals and Controls.

Striatal-specific *Foxp1* knockdown animals also performed press-sequences similarly to Controls. There were no differences in the organisation of press-sequences or the speed at which they were performed, which could indicate a deficit in fine motor-skills. Furthermore, the variability of pressing was normal suggesting that automatisation of motor-skills is not altered.

The ability to learn novel motor-skills is linked to the dorsal striatum (Costa *et al.* 2004), where Foxp1 deletion was substantial in striatal-specific Foxp1 knockdown mice. Taken together, data from the accelerating rotarod and the lever-pressing task suggest that Foxp1 does not play a major role in motor-skill learning, except perhaps at early stages. Motor-skill learning deficits have not been reported, and have in some cases not been tested for, in other Foxp1 mouse models (Bacon *et al.* 2015; Araújo *et al.* 2015) but gross motor delay has been reported in a subset of people carrying *Foxp1* disruptions (Bacon *et al.* 2012).

4.3. Foxp1 and social behaviour

Deficits in social interaction are primary diagnostic indicators of autism. Nevertheless, no differences were seen in sociability or preference for social novelty in striatal-specific Foxp1 knockdown mice compared to Controls in the 3-chamber task. However, these data are difficult to interpret because there was significant *Foxp1* expression in the ventral striatum of these animals, a region known to be important for social motivation and reward. Interestingly, preliminary data suggest that global *Foxp1* heterozygous animals also behave normally when performing the 3-chamber task (Ghita, L. personal communication). There are alternative behavioural tasks available to examine other aspects of social behaviour in mice, for example direct interaction, tube test, water T-maze or vocalisations but it should also be kept in mind that studies in mice may not be able to entirely replicate complex human social behaviour.

4.4. Potential Foxp1 and Foxp2 cooperative functions

Recent studies of FoxP family proteins in humans and rodents have significantly increased the understanding of their neuronal functions. Although disruptions of *Foxp1* and *Foxp2* cause autism spectrum disorders and a rare speech and language disorder respectively, these proteins are known to interact and may function cooperatively in brain regions where they are co-expressed such as the striatum. To investigate this mice with global heterozygous deletion of Foxp1 and global heterozygous deletion of Foxp2 (*Foxp1-Δ11-12* and *Foxp2-S321X* lines) were intercrossed. Clear differences are seen in dHet mice compared to controls, Het1 and Het2 animals on the accelerating rotarod task, not only in the latency to fall but also in the learning rate. Although these data are consistent with a cooperative role for Foxp1 and Foxp2 in motor-skill learning, at this stage it is not possible dismiss the possibility that we are affecting two pathways that independently contribute to motor-skill learning.

4.5. Future perspectives

Although *Foxp1* deletion was not as expected initially, in which mice revealed a knockdown of *Foxp1* rather than a knockout, the striatal-specific Foxp1 knockdown line allows to observe some interesting characteristics, which should be studied with different mouse models.

Deleting the *Foxp1* gene in adulthood with viral injections in the nucleus accumbens, a region related to rewarding experiences and motivation, has been doing to investigate social behaviour in these animals.

The analyses of motor and social behaviour in offspring from the *Foxp1-Δ11-12/+* and *Foxp2-S321X/+* with a view to investigating functional cooperation between Foxp1 and Foxp2 in the future also has been performing.

References

American Psychiatric Association. 1980. *Diagnostic and Statistical Manual of Mental Disorders*. Third Edition. Washington, DC: The American Psychiatric Association. doi:10.1017/CBO9781107415324.004.

Araújo, D., Anderson A. *et al.* 2015. 'FoxP1 Orchestration of ASD-Relevant Signaling Pathways in the Striatum'. *Genes & Development*, 29 (20): 2081–2096. doi:10.1101/gad.267989.115.6.

Bacon, C. and Rappold, G. 2012. 'The Distinct and Overlapping Phenotypic Spectra of FOXP1 and FOXP2 in Cognitive Disorders'. *Human Genetics* 131 (11): 1687–1698. doi:10.1007/s00439-012-1193-z.

Bacon, C., Schneider, M. *et al.* 2015. 'Brain-Specific *Foxp1* Deletion Impairs Neuronal Development and Causes Autistic-like Behaviour'. *Molecular Psychiatry* 20 (5): 632–639. doi:10.1038/mp.2014.116.

Boat, T., Wu, J. *et al.* 2015. *Mental Disorders and Disabilities Among Low-Income Children*. Washington, DC: The National Academies Press. doi:10.17226/21780.

Chen, J., Peñagarikano, O. *et al.* 2015. 'The Emerging Picture of Autism Spectrum Disorder: Genetics and Pathology'. *Annual Review of Pathology Mechanisms of Disease* 10 (1): 111–144. doi:10.1146/annurev-pathol-012414-040405.

Costa, R., Cohen, D. *et al.* 2004. 'Differential corticostriatal plasticity during fast and slow motor skill learning in mice'. Current Biology 14 (13): 1124-1134. doi:10.1016/j.cub.2004.06.053

Dang, M., Yokoi, F. *et al.* 2006. 'Disrupted Motor Learning and Long-Term Synaptic in Mice Lacking *NMDAR1* in the Striatum'. *PNAS* 103 (41): 15254–15259. doi:10.1073/pnas.0601758103

DiLuca, M. and Olesen, J. 2014. 'The Cost of Brain Diseases: A Burden or a Challenge?'. *Neuron* 82 (6): 1205–1208. doi:10.1016/j.neuron.2014.05.044.

Elsabbagh, M., Divan, G. *et al.* 2012. 'Global Prevalence of Autism and Other Pervasive Developmental Disorders'. *Autism Research* 5 (3): 160–179. doi:10.1002/aur.239.

Feng, X., Ippolito, G. *et al.* 2010. 'Foxp1 Is an Essential Transcriptional Regulator for the Generation of Quiescent Naive T Cells during Thymocyte Development'. *Blood* 115 (3): 510–518. doi:10.1182/blood-2009-07-232694.

Ferland, R., Cherry, T. *et al.* 2003. 'Characterization of Foxp2 and Foxp1 mRNA and Protein in the Developing and Mature Brain'. *The Journal of Comparative Neurology* 460 (2): 266–279. doi:10.1002/cne.10654.

French, C., Groszer, M. *et al.* 2007. 'Generation of Mice with a Conditional *Foxp2* Null Allele'. *Genesis* 45 (7): 440–46. doi:10.1002/dvg.

French, C., Jin, X. *et al.* 2012. 'An Aetiological *Foxp2* Mutation Causes Aberrant Striatal Activity and Alters Plasticity during Skill Learning'. *Molecular Psychiatry* 17 (11): 1077-1085. doi:10.1038/mp.2011.105.

Fröhlich, H., Rafiullah, R. *et al.* 2017. 'Foxp1 Expression Is Essential for Sex-Specific Murine Neonatal Ultrasonic Vocalization'. *Human Molecular Genetics* 26 (8): 1511–1521. doi:10.1093/hmg/ddx055.

Fuccilo, M. 2016. 'Striatal Circuits as a Common Node for Autism Pathophysiology'. *Frontiers in Neuroscience* 10: 27 doi:10.3389/fnins.2016.00027

Gage, G., Kipke, D. *et al.* 2013. 'Whole Animal Perfusion Fixation for Rodents', *Journal of Visualized Experiments*. doi:10.3791/3564.

Geschwind, D. and State, M. 2015. 'Gene Hunting in Autism Spectrum Disorder: On the Path to Precision Medicine'. *The Lancet Neurology* 14 (11): 1109–1120. doi:10.12788/j.sder.0080.

Golson, M. and Kaestner, K. 2016. 'Fox Transcription Factors: From Development to Disease'. *Development* 143 (24): 4558–4570. doi:10.1242/dev.112672.

Groszer, M., Keays, D. *et al.* 2008. 'Impaired Synaptic Plasticity and Motor Learning in Mice with a Point Mutation Implicated in Human Speech Deficits'. *Current Biology* 18 (5): 354–362. doi:10.1016/j.cub.2008.01.060.

Guan, C., Ye, C. *et al.* 2010. 'A Review of Current Large-Scale Mouse Knockout Efforts'. *Genesis* 48 (2): 73–85. doi:10.1002/dvg.20594.

Hannenhalli, S., and Kaestner, K. 2009. 'The Evolution of Fox Genes and Their Role in Development and Disease'. *Nature Reviews Genetics* 10 (4): 233–240. doi:10.1016/j.micinf.2011.07.011.Innate.

Jin, X. and Costa, R. 2010. 'Start/stop Signals Emerge in Nigrostriatal Circuits during Sequence Learning.' *Nature* 466 (7305): 457–462. doi:10.1038/nature09263.

Kalat, J. 2012. *Biological Psychology*. Eleventh Edition. Belmonte CA: Wadsworth Publishing.

Kanner, L. 1943. 'Autistic Disturbances of Affective Contact'. *Nervous Child* 35 (4): 100-136. doi:10.1105/tpc.11.5.949.

Klaus, A., Martins, G. *et al.* 2017. 'The Spatiotemporal Organization of the Striatum Encodes Action Space'. *Neuron* 95 (5): 1171–1180. doi:10.1016/j.neuron.2017.08.015.

Koralek, A., Jin, X. *et al.* 2012 'Corticostriatal plasticity is necessary for learning intentional neuroprosthetic skills'. *Nature* 483 (7389): 331-335. doi:10.1038/nature10845

Lai, C., Fisher, S. *et al.* 2001. 'A Forkhead-Domain Gene Is Mutated in a Severe Speech and Language Disorder'. *Nature* 413 (6855): 519-523. doi:10.1038/35097076.

Lanciego, J., Luquin, N. *et al.* 2012. 'Functional Neuroanatomy of the Basal Ganglia'. *Cold Spring Harbor Perspectives in Medicine* 2 (12): 1–20. doi:10.1101/cshperspect.a009621.

Marzluff, J., Miyaoka, R. *et al.* 2012. 'Brain Imaging Reveals Neuronal Circuitry Underlying the Crow's Perception of Human Faces'. *Proceedings of the National Academy of Sciences* 109 (39): 15912–15917. doi:10.1073/pnas.1206109109

Matthews, G. 2001. *Neurobiology: Molecules, Cells and Systems*. Second Edition. Malden: Blackwell Science, Inc.

Mendoza, E. and Scharff, C. 2017. 'Protein-Protein Interaction Among the FoxP Family Members and Their Regulation of Two Target Genes, *VLDLR* and *CNTNAP2* in the Zebra Finch Song System'. *Frontiers in Molecular Neuroscience* 10 (112): 1–15. doi:10.3389/fnmol.2017.00112.

Miller, L.. 2010. 'Analyzing Gels and Western Blots with ImageJ'. *Lukemiller.org*. http://lukemiller.org/index.php/2010/11/analyzing-gels-and-western-blots-with-image-j/.

Morgan, A., Fisher, S. *et al.* 2016. '*FOXP2*-Related Speech and Language Disorders'. *Gene Reviews*. https://www.ncbi.nlm.nih.gov/books/NBK368474/.

Moy, S., Nadler, J. *et al.* 2004. 'Sociability and preference for social novelty in five inbred strains: an approach to assess autistic-like behavior in mice'. Genes Brain Behavior 3 (5): 287–302. doi: 10.1111/j.1601-1848.2004.00076.x.

Moy, S., Nadler, J. et al. 2007. 'Mouse Behavioral Tasks Relevant to Autism: Phenotypes of Ten Inbred Strains'. *Behavioral Brain Research* 176 (1): 4–20. doi:10.1016/j.bbr.2006.07.030.

Myers, A., Souich C. *et al.* 2017. 'FOXP1 Haploinsufficiency: Phenotypes beyond Behavior and Intellectual Disability?' *American Journal of Medical Genetics* doi:10.1002/ajmg.a.38462.

Oliveira, G., Ataíde, A. *et al.* 2007. 'Epidemiology of Autism Spectrum Disorder in Portugal: Prevalence, Clinical Characterization, and Medical Conditions'. *Developmental Medicine & Child Neurology Child Neurology* 49 (10): 726–733. doi:10.1111/j.1469-8749.2007.00726.x.

Purves, D., Augustine, G. *et al.* 2012. *Neuroscience*. Fifth Edition. Sunderland: Sinauer Associates

Skarnes, W., Rosen, B. *et al.* 2011. 'A Conditional Knockout Resource for the Genome-wide Study of Mouse Gene Function'. *Nature* 474 (7351): 337–342. doi:10.1038/nature10163.A.

Sollis, E., Graham, S. *et al.* 2015. 'Identification and Functional Characterization of *de novo FOXP1* Variants Provides Novel Insights into the Etiology of Neurodevelopmental Disorder'. *Human Molecular Genetics* 25 (3): 546–557. doi:10.1093/hmg/ddv495.

Sollis, E., Deriziotis, P. *et al.* 2017. 'Equivalent Missense Variant in the *FOXP2* and *FOXP1* Transcription Factors Causes Distinct Neurodevelopmental Disorders'. *Human Mutation*, doi:10.1002/humu.23303.

Squire, L., Bloom, F. *et al.* 2013. *Fundamental Neuroscience*. San Diego: Elsevier, Academic Press.

Tamura, S., Morikawa, Y. *et al.* 2003. 'Expression Pattern of the Winged-Helix/forkhead Transcription Factor Foxp1 in the Developing Central Nervous System'. *Gene Expression Patterns* 3 (2): 193–197. doi:10.1016/S1567-133X(03)00003-6.

Tamura, S., Morikawa, Y. *et al.* 2004. 'Foxp1 Gene Expression in Projection Neurons of the Mouse Striatum'. *Neuroscience* 124 (2): 261–267. doi:10.1016/j.neuroscience.2003.11.036.

Tecuapetla, F., Matias, S. *et al.* 2014. 'Balanced Activity in Basal Ganglia Projection Pathways Is Critical for Contraversive Movements'. *Nature Communications* 5: 4315. doi:10.1038/ncomms5315.

Teramitsu, I., Kudo, L. *et al.* 2004. 'Parallel *FoxP1* and *FoxP2* Expression in Songbird and Human Brain Predicts Functional Interaction'. *The Journal of Neuroscience* 24 (13): 3152–3163. doi:10.1523/JNEUROSCI.5589-03.2004.

Vargha-Khadem, F., Gadian, D. *et al.* 2005. '*FOXP2* and the Neuroanatomy of Speech and Language'. *Nature Reviews Neuroscience* 6 (2): 131–138. doi:10.1038/nrn1605.

Vernes, S., Oliver, P. *et al.* 2011. 'FOXP2 Regulates Gene Networks Implicated in Neurite Outgrowth in the Developing Brain'. *PLoS Genetics* 7 (7). doi:10.1371/journal.pgen.1002145.

Vicente, A., Galvão-Ferreira, P. *et al.* 2016. 'Direct and Indirect Dorsolateral Striatum Pathways Reinforce Different Action Strategies'. *Current Biology* 26 (7): 267–269. doi:10.1016/j.cub.2016.02.036.

Vogel, A., Gutmann, D. *et al.* 2017. 'Neurodevelopmental Disorders in Children with Neurofibromatosis Type 1'. *Developmental Medicine & Child Neurology*. doi:10.1111/dmcn.13526.

Wang, B., Weidenfeld, J. *et al.* 2004. '*Foxp1* Regulates Cardiac Outflow Tract, Endocardial Cushion Morphogenesis and Myocyte Proliferation and Maturation'. *Development* 131 (18): 4477–4487. doi:10.1242/dev.01287.

Watkins, K., Vargha-Khadem, F. *et al.* 2002. 'MRI Analysis of an Inherited Speech and Language Disorder: Structural Brain Abnormalities'. *Brain* 125 (3): 465–478. doi:10.1093/brain/awf057.

World Health Organization 2013. 'Autism Spectrum Disorders & Other Developmental Disorders. From Raising Awareness to Building Capacity'. Geneva, Switzerland

Yang, M., Silverman, J. *et al.* 2011. 'Automated Three-Chambered Social Approach Task for Mice'. *Current Protocols in Neuroscience* 8: 8.26. doi:10.1002/0471142301.ns0826s56.

Zhang, J., Zhao, J. *et al.* 2012. 'Conditional Gene Manipulation: Cre-Ating a New Biological Era'. *Journal of Zhejiang University Science B* 13 (7): 511–524. doi:10.1631/jzus.B1200042.